

**ASSESSING SEDIMENT DYNAMICS AND CHANNEL BAR RESPONSE
IN THE BRAZOS RIVER NEAR GLEN ROSE, TEXAS**

by

MAARTJE L.K. MELCHORS

Bachelor of Arts, 2008
University of Vermont
Burlington, VT

**Submitted to the Graduate Faculty of the
College of Science and Engineering
Texas Christian University
In partial fulfillment of the requirements
for the degree of**

Master of Science

May 2012

ACKNOWLEDGEMENTS

A special thanks to my committee members, Dr. Michael Slattery for his guidance, expertise and field support throughout this project. I would also like to thank Mrs. Tamie Morgan, for being an excellent mentor in GIS, and Dr. John Holbrook for his input and recommendations. I acknowledge the remaining TCU Geology faculty for giving me the chance to take part in the program. I will always be grateful for this opportunity.

A sincere thank you to my field assistant Peyton Lisenby for the days spent at the Brazos River, and for all the heavy lifting. I am truly indebted to you. Finally, to my family, James and Emma, thank you for your patience and unwavering support.

TABLE OF CONTENTS

ACKNOWLEDGEMENTS.....	ii
LIST OF FIGURES.....	iv
LIST OF TABLES.....	vi
CHAPTER 1: INTRODUCTION.....	1
CHAPTER 2: LITERATURE REVIEW	4
River Channel Plan Form.....	4
Sediment Transport.....	5
Channel Bar Formation.....	8
Fluvial Geomorphology and GIS.....	10
CHAPTER 3: STUDY AREA	11
CHAPTER 4: METHODOLOGY.....	16
USGS Water Data.....	16
Sediment Sampling.....	17
Channel Bar Surveys	20
Sediment Analysis.....	22
GIS Analysis.....	24
CHAPTER 5: RESULTS AND DISCUSSION.....	26
Historic Flow Conditions.....	26
Analysis of historic photography	28
Channel Bar Surveys	38
Interpretation of survey transects.....	46
Establishing a sediment record	52
CHAPTER 6: CONCLUSION	61
REFERENCES.....	64
APPENDIX.....	67
VITA	
ABSTRACT	

LIST OF FIGURES

Figure 1. Relationship between the entrainment, transport and deposition of material of varying particle sizes described by Hjülstrom (1939)	6
Figure 2. Channel bar development as described by Leopold and Wolman (1957).....	9
Figure 3. River Basin Map of Texas showing the extent of 13 river basins.....	11
Figure 4. Overview of study area on the Brazos River in Somervell County, Texas.....	13
Figure 5. Downstream view of channel bars from FM 200 Bridge	14
Figure 6. Upstream view of channel bars from FM 200 Bridge	14
Figure 7. Aerial view of study site showing location of FM 200 Bridge	14
Figure 8. Analysis of mean monthly Q for pre-and post-impoundment flow conditions.	16
Figure 9. Sediment sampling stations and gaging station on FM 200 Bridge	18
Figure 10. Channel cross section, completed in October 2011, showing locations of sampling stations across the FM 200 Bridge	19
Figure 11. Location of permanent control points along the study site.....	22
Figure 12. Flow duration curves showing flow trends before and after construction of the dam.....	27
Figure 13. Locations of individual channel bar complexes along study reach.....	28
Figure 14. Visual comparison of channel configuration and bar locations established from historic photography (1949 to 1984).....	29
Figure 15. Inundation curve used to establish corrected channel bar areas.....	31
Figure 16. Comparison of channel bar area across the reach for each of the historic images	33
Figure 17. Fluctuations in mean annual discharge rates at the study site 1941 to 2010...	35
Figure 18. Channel scour for post construction years observed through photographic analysis.....	36
Figure 19. Comparison between channel bar locations 1966 to 1976	37
Figure 20. Comparison between channel bar locations 1976 to 1984	37

Figure 21. Discharge trends for February 2011 to March 2012 compared with rates of precipitation	39
Figure 22. April 2011 Terrain data model showing range of elevation across the mid channel bar	41
Figure 23. Overlay of April 2011 and October 2011 surveys showing areas of scour and deposition	42
Figure 24. Overlay of completed surveys April 2011, October 2011 and March 2012....	43
Figure 25. Location of transects for October 2011 and March 2012 surveys.....	46
Figure 26. Comparison of 6 transects across the channel bar showing topography change from October 2011 to March 2012	48
Figure 27. Overlay of March 2012 TIN (shown in green) and October 2011 TIN (shown in brown). Elevations are vertically exaggerated to show detail.	51
Figure 28. August 2011 hydrograph showing the relationship between discharge and precipitation. Sediment sampling time is marked by dashed line.....	53
Figure 29. October 2011 hydrograph, sampling time is marked by dashed line	54
Figure 30. January 2012 hydrograph showing sediment sampling times with dashed lines	54
Figure 31. Correlation of suspended sediment concentration and discharge.....	55
Figure 32. A hysteresis curve for the January 2012 storm event indicates that SSC peaked around $200 \text{ m}^3\text{s}^{-1}$	57
Figure 33. Relationship between suspended sediment flux and discharge	58
Figure 34. Relationship between turbidity measurements and physical suspended sediment samples obtained during field sampling	58
Figure 35. Bedload transportation rates according to variations in Q	60

LIST OF TABLES

Table 1. Revised area calculations for channel bar 1-A. Calculations may be compared with contemporary field surveys.....	31
Table 2. Planform area measurements showing original and revised calculations for the entire bar complex.....	44
Table 3. Revised planform area calculations separating upper and lower portions of the channel bar.....	44
Table 4. Planform area measurements for lower channel bar to include March 2012 survey.....	46

CHAPTER 1: INTRODUCTION

As population grows rapidly, an increasing stress is being placed on the nation's water resources. The implementation of dams provides many communities across the country with irrigation capabilities, the generation of hydroelectric power, a means of flood protection, and potentially increased recreational opportunities. However, to date widespread observations have been made on undesirable changes associated with dams and impoundments, especially regarding the downstream health of a river channel (Kondolf, 1997; Slattery et al., 2010; Wellmeyer et al., 2004). Under natural conditions, rivers carry sediment from eroding uplands to depositional areas near the coast. The construction of dams interrupts the continuity of this transport system by trapping sediments in reservoirs and creating sediment-starved water downstream. This flow, coined with the term 'hungry water', has the capability to erode and incise channels and potentially introduces large amounts of sediment into downstream reaches (Kondolf, 1997; Phillips et al., 2004). Additionally, fragmentation of a river system induces changes in the hydrologic flow regime by reducing the magnitude and frequency of the maximum and minimum flow. Low flow levels are generally responsible for the deposition of sediment and are most likely to occur during periods of reduced precipitation. Peak flows, on the other hand, induce higher rates of material transport and are responsible for flushing excess storage within the system. Material entrainment and transport is largely related to a river's specific stream power which is determined by the channel slope and discharge rate. If the flow regime is in general equilibrium, both maximum and minimum discharge rates are attained, sediment is deposited and subsequently removed causing no significant net change in channel morphology (Ritter, 2002). The introduction of a dam

often reduces the magnitude of the maximum flow in downstream reaches. Numerous studies have shown a lowering of sediment transport rates in these areas resulting in a reduction of channel width due to increased sediment storage within the channel (Kondolf, 1997; Vörösmarty et al, 2003; Walling and Fang 2003). In general rivers are capable of adjusting hydraulic parameters to accommodate changes in discharge and sediment load by establishing short-term quasi equilibrium states (Richards 1982). However, as channel instability increases an undesirable channel shift may occur. Through continual monitoring, a relationship may be established between sediment dynamics and the rate of change in channel morphology.

This thesis presents the results of a one-year study examining sediment transport rates and channel bar morphology in the Brazos River near Glen Rose, Texas. The main objectives of the study are to:

- (1) Utilize Geographic Information Systems (GIS) and historic aerial photography to understand changes in channel and bar morphology pre and post dam construction in a reach of the Brazos River near Glen Rose;
- (2) Determine short-term change in bar morphology through the monitoring of bar formations over a one year study period (February 2011 – March 2012) with the use of repeated ground surveys;
- (3) Understand suspended sediment dynamics along the reach by establishing a relationship between turbidity measurements and suspended sediment samples collected over a range of flow events;

(4) Gain a better understanding of the variability in bedload transport at the study site.

This study may aid in determining how the Brazos River near Glen Rose has responded to the construction of De Cordova Bend Dam at Lake Granbury, and how current conditions in sediment dynamics are influencing the general bar morphology. For communities which rely heavily on the Brazos River, it is important to understand the implications of increased water allocation on the river's overall health and navigability.

CHAPTER 2: LITERATURE REVIEW

Responsible water resource management will become increasingly important in the future as population continues to grow rapidly. The formation of reservoirs allows for the capture and storage of storm water which may subsequently serve as a drinking water source. A major drawback in the continued development of dams lies with the increased fragmentation of fluvial systems causing disruptions in the natural hydrologic cycle. These disruptions are manifested by changes in the discharge regime as dams diminish seasonal peak flow events and interrupt sediment transport.

River Channel Plan Form

The degree of erosion and transport of sediment within a river depends largely on the balance between driving and resisting forces. Ritter (2002) suggests that it can be described by the difference between the potential energy produced by the flow and the energy consumed by the resistance to the flow. A river accommodates changes in sediment load and discharge by adjusting its channel pattern, or plan form, in various ways. Adjustments of equilibrium may occur over varying timescales depending on the mobility of channel forming sediments. The original classification scheme proposed by Leopold and Wolman (1957) established three patterns: straight, meandering and braided. A wider range of river patterns was determined by Schumm (1981) who combined traditional channel patterns with the specific sediment load carried by the river. The transition from straight to meandering streams is determined by sinuosity. In general, straight reaches are characterized by accumulated bed material positioned successively on opposite sides of the channel. The thalweg, the path of deepest and fastest flow, migrates back and forth between the banks. If the river channel contains a poorly sorted sediment

load, the channel bed will develop a series of pools and riffles signifying areas of scouring and deposition. Over time these structures will allow for meander patterns to be established. In a natural state, meanders migrate by eroding banks of outside bends and depositing material on inside bends. They may continue to grow until a cutoff occurs. The rates of erosion and deposition ultimately determine the maintained channel pattern (Best et al., 2003; Gilvear et al., 2000; Ritter, 2002).

Sediment Transport

A river's sediment load is divided into suspended load and bedload. Suspended load is comprised of fine sand, silt and clay sized material that is transported in the water column above the bed. Ritter (2002) states that in many rivers suspended load is comprised completely of silt to clay-sized material. Disturbance within the water column allows for the material to remain in suspension, and therefore the amount of suspended sediment is directly proportional to the degree of turbulence. Material that makes up the suspended load most often originates from channel banks and may travel long distances downstream without stages of deposition (Hudson, 1997). Bedload, on the other hand, is composed of very coarse sand, to gravel to cobble sized material. Due to increased size and weight it is rolled along the bed rather than transported in suspension (Hudson, 1997; Ritter, 2002). Downstream transport is characterized by movement over short distances. The majority of bedload transport occurs during high discharge events when flow becomes exceedingly turbulent. As discharge rates fluctuate, a sediment particle may be part of the suspended load or bedload at any given time. The term washload was introduced to describe small particles which remain in suspension and due to their size are absent from the bed. Washload may be compared to bed material load which

describes material found in abundance on the bed. The concentration of the washload is primarily a function of supply as most rivers have the transporting power to move this material. Ritter (2002) suggests that the relationship between washload and discharge is therefore poorly defined. Coarse sediment should show a stronger relationship between concentration and discharge.

To initiate sediment transport a particle must first experience entrainment. The degree of entrainment depends on the critical bed velocity as well as the critical shear velocity, or erosive power of the flow. Hjülstrom (1939) described the transport and deposition of material according to particle size and velocity. Figure 1 shows that a relatively low mean velocity is required to transport silt to fine sands. Additionally, for fines the entrainment and settling curves show a significant separation. This suggests that a substantial decrease in mean velocity may not cause material to fall out of suspension. Coarser grained material requires a higher mean velocity to initiate entrainment. Furthermore, the spacing between the entertainment and settling curves suggest that a small decrease in mean velocity may cause deposition of the material.

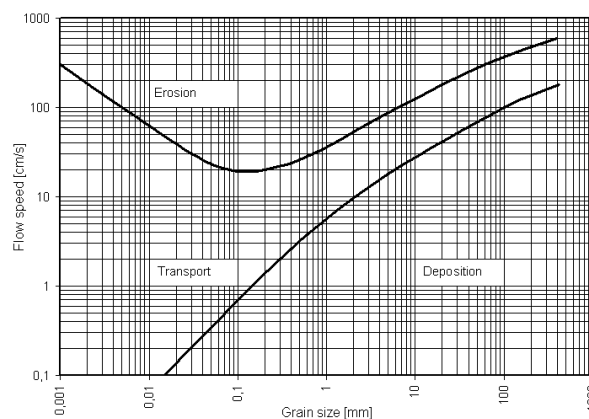


Figure 1. Relationship between the entrainment, transport and deposition of material of varying particle sizes described by Hjülstrom (1939)

A second factor influencing sediment entrainment is the specific critical shear stress exerted by the flow. Critical shear stress (Equation 1), τ_c , is described as the relationship between the specific weight of water, γ , the hydraulic radius, R , and the channel slope, S .

$$\tau_c = \gamma RS$$

This determines the downslope component of fluid weight exerted on a particle. Due to the nature of the relationship, a direct increase in the flow's critical shear stress is expected with an increase in hydraulic radius or channel slope (Ritter, 2002). Wolman and Miller (1960) suggested that continued sediment transport primarily occurs during intermediate events of high frequency, with a variation in maximum transport rates existing between different climates. Comparisons between semi-arid and humid environments show that high flow events have a greater impact in semi-arid environments due to greater sediment yield from slopes. Annual precipitation and discharge rates will therefore largely determine the degree to which sediment is removed and deposited within such a system.

A more accurate determination of sediment transport can be made if a continuous discharge record is available. According to Richards (1982), a flow duration curve may be established to describe the rate of transport. This analysis establishes a cumulative percentage curve of the time each discharge is equaled or exceeded. A flow duration curve defines specific flows, such as median ($Q=50\%$) as well as high and low flows. If combined with a sediment rating curve it gives a relatively accurate indication of sediment transport rates across a range of discharges.

Channel Bar Formation

If a channel experiences an extensive degree of erosion it is classified as a degrading system. The opposite is true if a system is depositing material at a higher rate than erosion is removing; in this case it is said to be aggrading. Human activity may influence the rate of degradation and aggradation. In order for a river channel to remain in equilibrium it must have similar rates of erosion and deposition (Hooke, 1986; Rosgen, 1996). The equilibrium state (Equation 2) may be described as follows:

$$I - O = \Delta S$$

where I equals the total input to the system, and O describes the output. The difference between the input and output is ΔS , or the change in storage. This relationship suggests that if sediment input to the system exceeds sediment output there is a positive net change in storage (Ritter 2002). Hungry water found in the reaches below a dam has the increased the potential for scouring and erosion due to excess energy. Material from affected regions may be transported and deposited in reaches downstream and create areas of storage in the form of channel bars. A Leopold and Wolman study (1957), confirmed by Lisle (1982), determined that initiation of channel bar growth is due to deposition of coarse material that exceeds the river's ability for transport (Figure 2). Vertical bar aggradation and lateral growth occurs downstream. As water is forced around the newly formed structure, channel banks experience increase scour and may cause the channel to locally widen. A deepening of the channel bed lowers water levels allowing the channel bar to emerge as an island.

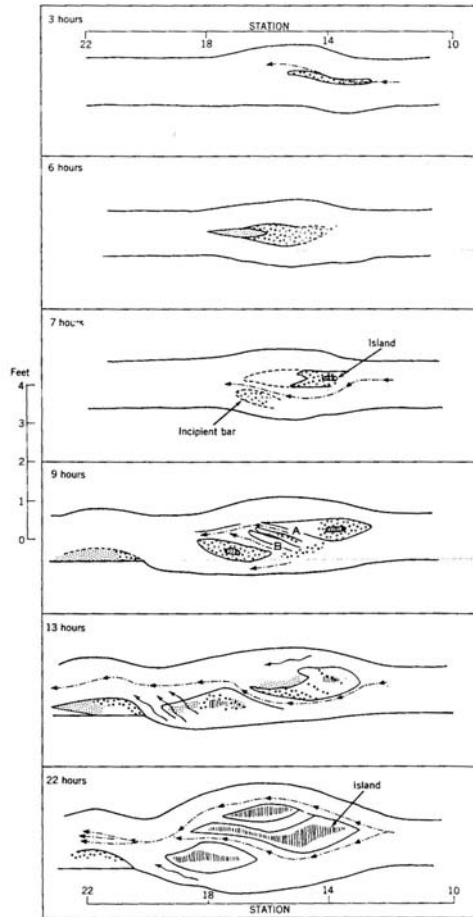


Figure 2. Channel bar development as described by Leopold and Wolman (1957)

Ashworth (2000) and Best et al. (2003) proposed a model under which mid channel bar growth occurs if a channel is experiencing significant erosion in upstream reaches. In this study, bar development occurred as local sediment supply increased due to erosion. Bed scour was initiated by convergent flow creating a local pool. As flow traveled out of this zone it diverged producing an area of deposition. Over time bar growth occurred through lateral accretion, eventually shifting the primary thalweg forcing the channel to widen to accommodate the divided flow. In the case of the Jamuna

River mentioned by Ashworth (2000), erosion of the channel banks due to the shift of the thalweg supplied within channel deposition for the downstream area of the bar.

Fluvial Geomorphology and GIS

Numerous topics in fluvial geomorphology investigate change over decadal time scales. Due to the nature of the discipline, Geographic Information Systems (GIS) serves as useful tool for understanding and mapping these changes (Eidse, 2005; Jacobson and Pugh, 1995). Widely used GIS applications are found in land cover assessment, forestry and natural resource management studies. For the purposes of fluvial geomorphology, changes in river planform and channel bar morphology may be determined with the use of GIS through the careful interpretation of historical maps, aerial photography or satellite imagery (Downward et al., 1994; Jordan et al. 2005; Marcus et al., 2003). If sufficient data is available, GIS offers a method of describing a river channel's morphology through time as it allows the user to capture and integrate boundaries of system and features. Using GIS as a tool for river planform change often limits the data sources to no more than 100 years before the present as this marks a period during which accurate large scale maps (1:10,000) became available (Marcus, 2002). The primary advantage of adopting a GIS based approach includes the ability for direct digitization of boundaries from source documents, which allows for the quantitative analysis of linear and areal displacement. If additional interpretation is required, the derived digital measurements can be exported into statistical software packages. It must be taken into consideration that the use of maps or imagery at large scales potentially introduces measurement error, especially in less dynamic systems where change over time is subtle (Downward et al., 1994).

CHAPTER 3: STUDY AREA

Texas is subdivided into 13 major river basins (Figure 3). The individual basins vary in shape, length and stream pattern due to the differences in geology, topography, vegetation and precipitations across the region. The Brazos River Basin covers 15% of the state, or a total of 114,000 km². The river's headwaters originate in eastern New Mexico with the river mouth located in Freeport, Texas. As is true for many rivers across the United States, over the past century the Brazos River has become a highly fragmented system. There are currently 19 major reservoirs along the Brazos River, providing 26 billion liters of water each year to surrounding cities, agriculture and industry (Brazos River Authority).

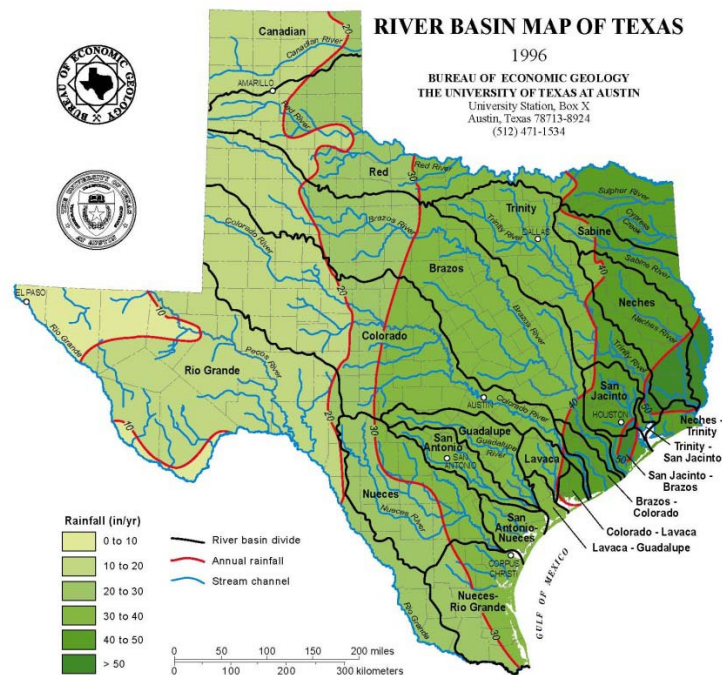


Figure 3. River Basin Map of Texas showing the extent of 13 river basins

Climate in north central Texas is humid subtropical with a wide temperature and precipitation range. Based on the River Basin Map of Texas it is estimated that the central Brazos River Basin receives on average 70 to 100 cm of precipitation annually. Substantial storm events, and therefore peak flow levels, tend to occur during the spring and fall. Generally, spring is characterized by high intensity and short duration storm events, whereas fall storm events are of lower intensity but longer duration. The reach of the Brazos River chosen for this study is located in Somervell County approximately 80 km southwest of Fort Worth, Texas (Figure 4). It is on the border between the upper and central Brazos River Basin, a region characterized by a wide and shallow meandering channel.

In this region, the Brazos River cuts the lower Cretaceous Glen Rose Limestone formation, a unit belonging to the Trinity Group. It consists of a series of shallow marine formations deposited during transgression and regression events. The Glen Rose Formation is characterized by alternating layers of limestone and marl limestone. When exposed to weathering processes, the different strengths of the alternating layers allows for the formation of stepped platforms which are commonly observed in the region (Epps, 1973). The study site is positioned approximately 40 river kilometers below De Cordova Bend Dam at Lake Granbury. Construction on this particular dam began in 1966 and was completed in 1969. Currently, Lake Granbury is operated by the Brazos River Authority and provides 170 million m³ of storage capacity for conservation of flood and storm waters (Brazos River Authority). The reach of the Brazos River chosen for this study is characterized by a wide, shallow and low gradient channel with prominent lateral channel bars (Figure 5 and Figure 6).

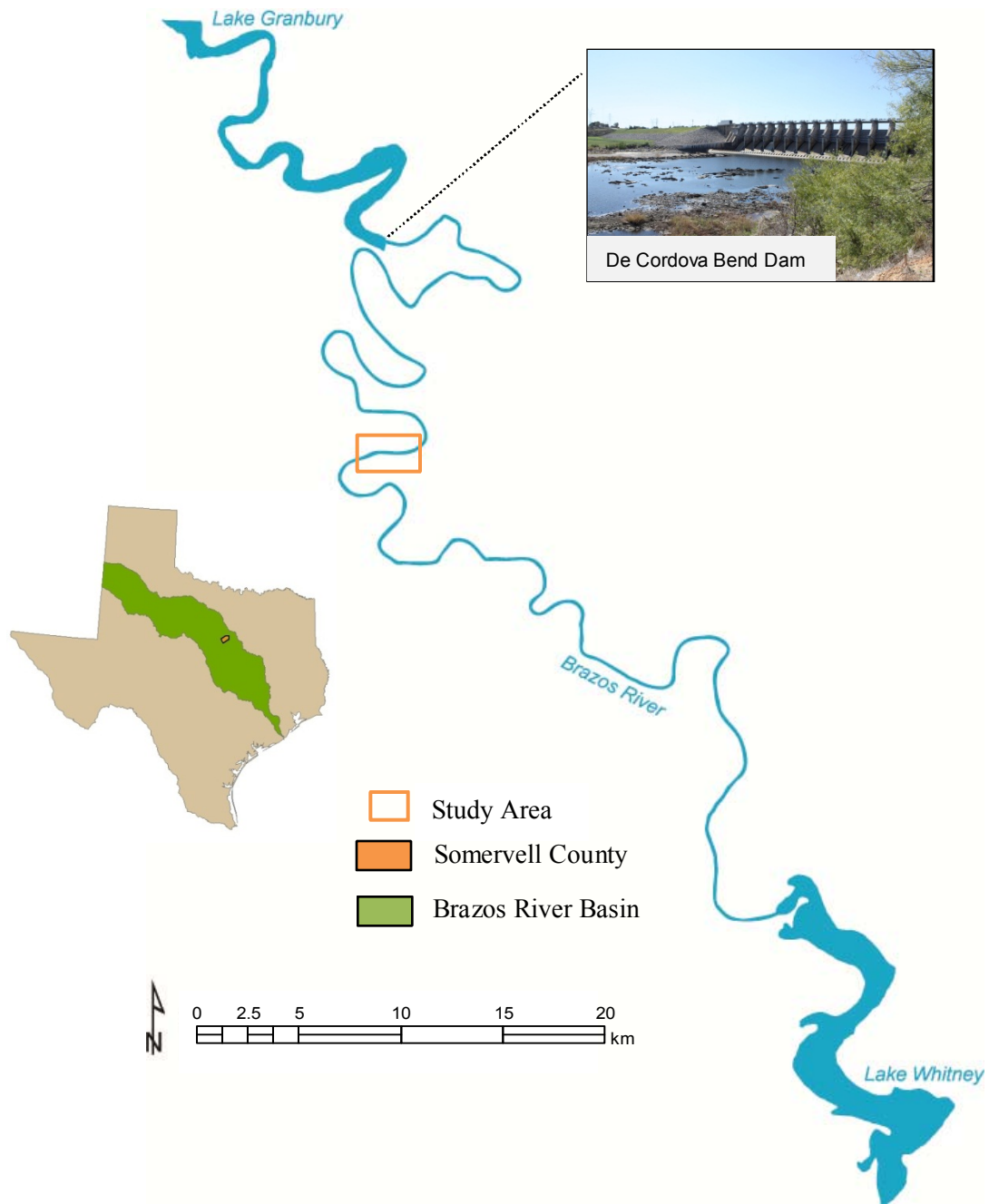


Figure 4. Overview of study area on the Brazos River in Somervell County, Texas



Figure 5. Downstream view of channel bars from FM 200 Bridge



Figure 6. Upstream view of channel bars from FM 200 Bridge



Figure 7. Aerial view of study site showing location of FM 200 Bridge

The river channel directly below the bridge measures approximately 85 m in width. Subsequently, channel bars at the study area measure 65 m in maximum width and 480 m in length with a range in elevation of 172.28 m to 172.83 m above sea level

(Figure 7). An average elevation below De Cordova Bend Dam was determined at 191 m above sea level; therefore there is a reduction in elevation of approximately 20 m between the reach below the dam and the study area. One of the primary considerations when selecting the specific study area was the presence of extensive mid channel bars as well as USGS Gaging Station 08091000 (Latitude 32°15'32'', Longitude 97°42'08''). In order to establish a relationship between channel bar morphology and sediment dynamics, an accurate discharge record must be available. USGS gaging station 08091000 marks the first station in the downstream reach below De Cordova Bend Dam. The station has maintained a continuous record on discharge rates, Q , in cubic feet per second (ft^3s^{-1}) dating back to 1923, gage height in feet (ft) dating to 1987 and real-time precipitation in inches (in). Precipitation data is made available for 120 days. For consistency throughout this project, all USGS data was converted according to the metric system.

CHAPTER 4: METHODOLOGY

USGS Water Data

The availability of a historic discharge record allowed for the comparison of flow trends at the study site pre- and post-dam construction. To establish an initial understanding of peak flow alteration due to the construction of the dam, mean monthly discharge rates were obtained for 1950 to 1980 (Figure 8). The record was subdivided into 3 individual intervals, spanning conditions before construction, as well as during and after construction. Under natural flow conditions, 1950 to 1960, this specific reach of the Brazos experienced peak flows during the spring and fall with the highest peak observed during the spring. A significant dampening of the spring peak is visible during the construction period. The post construction curve, 1970 to 1980, depicts a near elimination of seasonal peaks creating a more uniform annual flow.

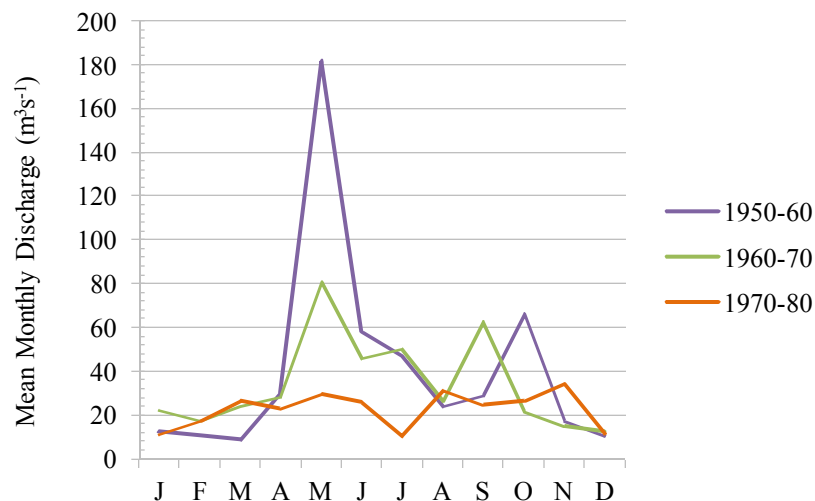


Figure 8. Analysis of mean monthly Q for pre-and post-impoundment flow conditions

A second method for establishing long-term flow trends is found with a flow duration curve. This curve captures the variability of flow rates with time and describes the relationship between average discharge rates and the frequency at which they are equaled or exceeded. Since stream flow rates vary daily and between seasons, it is pertinent that discharge measurements include a period spanning at least 30 years. To establish the curve, mean annual discharge data was ranked from 1 to 30 with ascending magnitudes. Exceedance probabilities (Equation 3) for each year were calculated as follows,

$$P = 100 * [m / (n + 1)]$$

where m equals the ranked position and n is the number of events for the period of record (Dingman, 2008). High flow events are generally represented in the 0 to 10% exceedance range, moist conditions between 10 to 40%, mid-range flow 40 to 60%, dry conditions 60 to 90%, and low flow events within the 90 to 100% exceedance range. For the study area it was determined that median discharge rates ($Q=50\%$) decreased from $36 \text{ m}^3\text{s}^{-1}$ pre-construction to $22 \text{ m}^3\text{s}^{-1}$ post construction (Figure 12).

Sediment Sampling

Field data collected over the study period (February 2011 to March 2012) aimed at understanding sediment flux at the cross section of the FM 200 Bridge, and combining the flux with the rate of response in channel bar morphology. Suspended sediment flux was determined in two parts; (i) by taking continuous turbidity readings, and (ii) obtaining suspended samples during storm events. A YSI600 OMS turbidity probe, measuring the optical clarity of the water, was installed along the bridge in the center of the flow. The instrument was programmed to take turbidity measurements every 3 hours

and remained onsite for the duration of the research period. To establish a relationship between turbidity readings and the actual quantity of sediment transported, suspended sediment samples were obtained over a range of flow conditions. It must be taken into account that suspended sediment concentrations vary from the water surface to the bed and laterally across the stream. Concentrations generally increase from a minimum at the water surface to a maximum at or near the bed (Kondolf 2003). To capture this variability a US D-74 depth integrating sampler was used at 5 individual bridge stations across the channel (Figure 9 and 10).

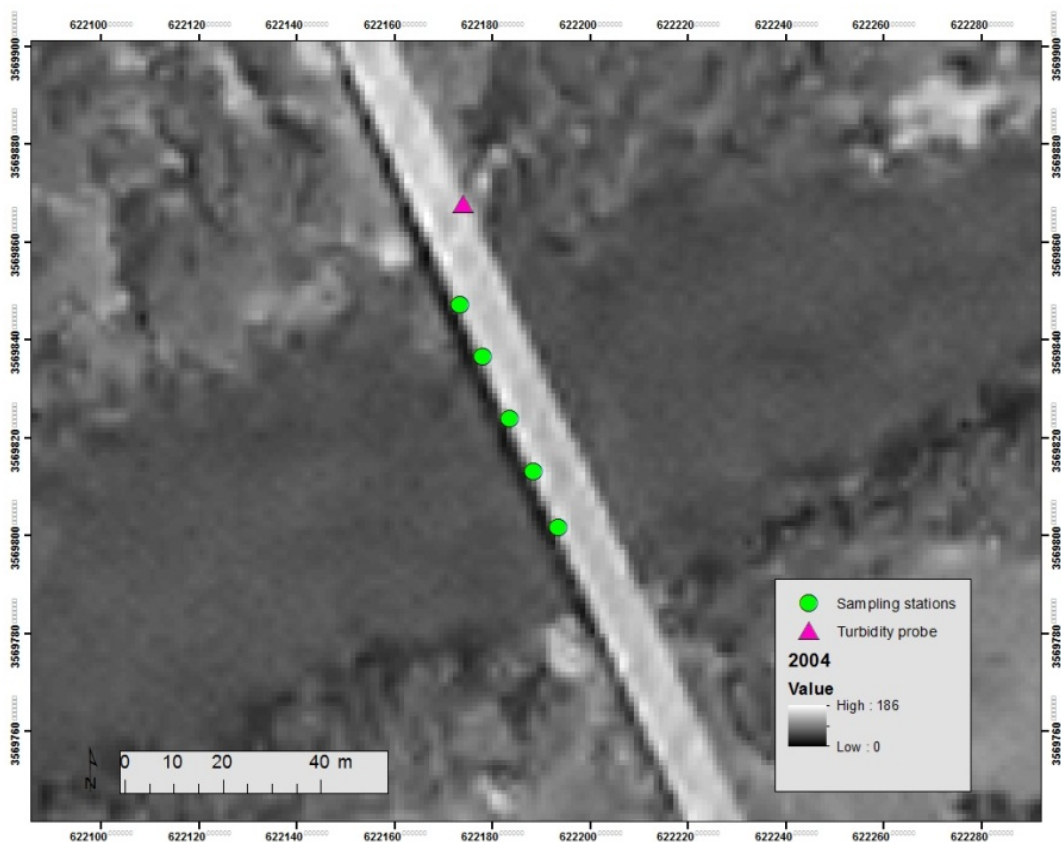


Figure 9. Sediment sampling stations and gaging station on FM 200 Bridge

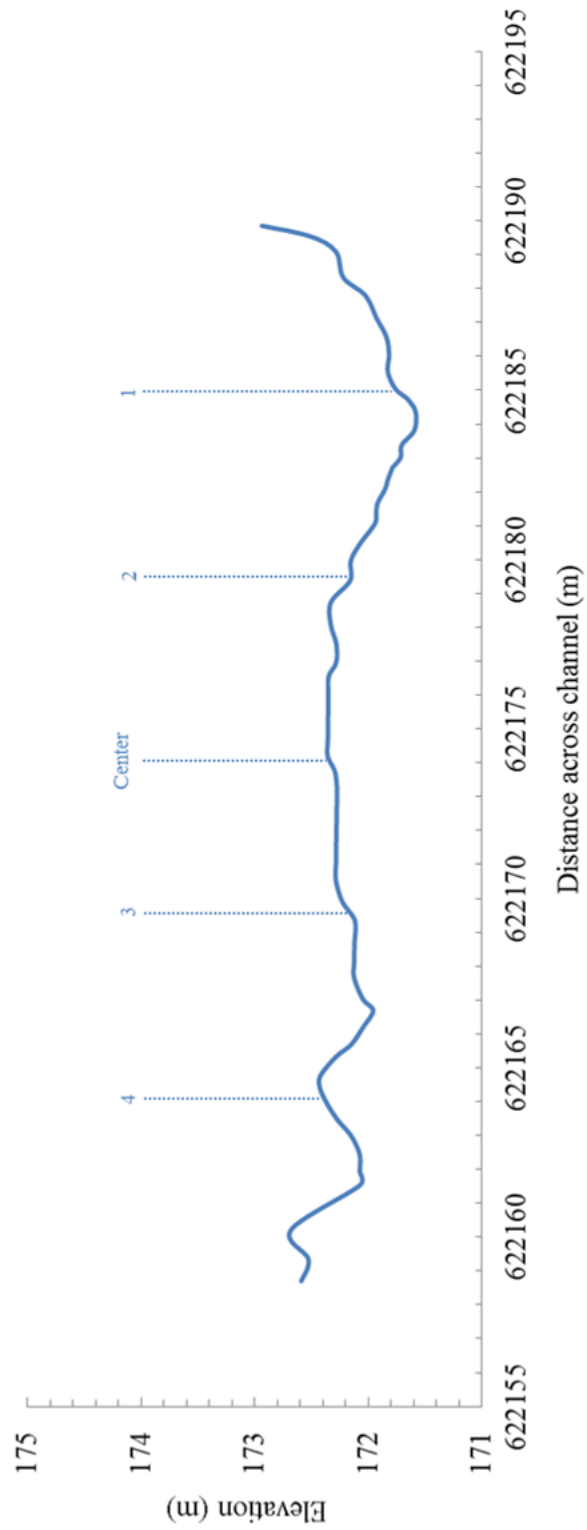


Figure 10. Channel cross section, completed in October 2011, showing locations of sampling stations across the FM 200 Bridge

A depth-integrated sampler is designed to continuously extract a water sample as it is lowered from the surface through the column and to the streambed. It is also returned at a constant rate of travel (Johnson 1997). A crane assembly was used to lower the sampler over the bridge. In addition to establishing suspended sediment flux, the study aimed at gaining a better understanding of bedload. To capture spatial variability, bedload measurements were also taken at each bridge station with the use of a Helley-Smith pressure difference sampler. This sampler obtains material ranging from coarse sand to gravel and is lowered onto the bed without creating disturbance. Bedload samples were collected in 0.25mm mesh bags over 5 minute sampling periods. Stubblefield et al. (2007) described that with the combination of actual sediment measurements and turbidity readings, a sediment rating curve can be produced to determine total annual sediment flux.

Channel Bar Surveys

Multiple channel bar surveys were completed over the study period to determine short-term change in bar morphology with seasonal fluctuations in discharge. An initial survey of the entire bar complex was completed in March 2011, which predates the arrival of significant spring discharge events. A Leica TS02 Flexline Total Station was used, and surveys were completed by walking the wetted perimeter of the channel bar while capturing a reading every 4 to 6 m. Readings of specific northing, easting and elevation for each point were stored in an AllegroCX hand held unit and later converted to shapefiles for use in ArcGIS. This method produced an accurate outline of the channel bar at a specific flow level and helped determine the areal extent of the structure in m². Each survey was completed with multiple transects to capture variability in topography

across the channel bar. Transects were re-surveyed over the study period to determine degree of aggradation or degradation after a significant storm event. Re-tracing of transects was completed with the use of a Trimble GeoXH unit, with a horizontal accuracy of 2.5cm (Trimble).

To obtain an accurate baseline survey, a Leica Scan Station c10 was used in April 2011. This technology is capable of capturing high-density point cloud data and imagery to an accuracy of 3mm per 100 meter. Long range scanning technology successively sends out thousands of pulsed beams of light while the system calculates the time of travel from departure to arrival back at the unit. Mirrors determine the beams horizontal and vertical angles to establish highly accurate x, y and z coordinates. The Leica Scan Station c10 has the ability to capture over 10,000 points per second (Leica). For this survey permanent control points were established at 9 individual locations, 2 control points are found at the FM 200 Bridge and 7 spanning the length of the channel bar (Figure 11). In order to maintain consistency throughout the project, control points were used in all subsequent surveys.



Figure 11. Location of permanent control points along the study site

The great accuracy of the Leica Scan Station c10 survey allows for the quantification of current sediment storage within the channel bar system. Additionally, the survey data may help to determine error associated with subsequent surveys completed with the Leica TS02 Flexline Total Station in October 2011 and March 2012. The repeated surveying method gives an indication of channel bar response to seasonal variability in discharge.

Sediment Analysis

All sediment samples were sealed onsite and returned to the lab for analysis. Suspended sediment samples were transferred to 100 ml containers and filtered to

separate silt and clay sized material from water. The filtration process was accomplished using a 0.45 μ m Millipore filter and a vacuum pump for suction. Due to the abundance of fine material and long filtration times, a prefilter was added. A Millipore prefilter eliminated clogging of the 0.45 μ m filter. Upon completion of the filtration process, membranes were dried in an oven at low heat for approximately 6 hours. This allowed for the evaporation of water trapped in the membrane leaving behind only clay and silt sized material. Filters were weighed and compared to their initial dry weight. The difference in weight signified the concentration of suspended sediment present in 100 ml of water collected. As with suspended sediment samples, bedload sample bags used in the Helley-Smith pressure difference bedload sampler were labeled and sealed onsite for further lab analysis. Samples containing a mixture of fine to medium sand and gravel were initially air dried and then transferred to secondary containers. A bedload weight for each individual sample was determined by weighing the container containing sediment and comparing it to the weight when empty.

GIS Analysis

In order to understand how channel planform and channel bars at the study area have responded to the construction of De Cordova Bend Dam, a series of historic photographs were obtained from TNRIS (Texas Natural Resource Information System) and P2 Energy Solutions spanning pre- and post-construction. Imagery was provided for the years 1949, 1959, 1966, 1976, and 1984. All acquired photos were provided in scanned format at 300dpi and required georeferencing. Accurate georeferencing for this type of study is crucial since the imagery is overlain to determine channel change between multiple years. This step was completed by using the georeferencing function in ArcMap (ESRI). A shapefile, also provided by TNRIS, containing an accurate roadmap for Somervell County was used as a reference. The shapefile projected in NAD_1983_UTM_Zone_14N and the unreferenced image were initially placed in a best fit, upon which ground control points could be determined to obtain a more accurate fit. Road intersections were the most efficient choice for ground control points, and 8-10 were selected for each image. The best possible combination of ground control points was attained to yield the lowest Root Mean Square error. The RMS error describes the standard deviation of differences in actual positions of ground control points and their calculated position after registration.

Upon completion of the rectification process, the channel banks and channel bar perimeters were digitized. This process was completed with the ArcMap Editor function. Individual shapefiles were created in ArcCatalog for the river channel outline and the channel bar outline for each imagery year. Digitization was completed by extensive zooming and accurate tracing of the specific features. Once the areas of interest were

rectified and digitized, ArcGIS gave precise measurements of length and area. This information was used when comparing areal change between successive years. To compare change in channel bar area, the exact discharge rate for the each of the images must be taken into account. The specific conditions will determine the degree to which the channel bar was either inundated or exposed. Each image was provided with an exact origination date. With this information, the mean daily discharge rate for each image could be obtained from the USGS gaging station record. Through careful monitoring of contemporary conditions, 0% inundation rates were established at $0.45 \text{ m}^3\text{s}^{-1}$, and 100% inundation at $32.85 \text{ m}^3\text{s}^{-1}$. An inundation curve helped determine the corrected bar areas for each of the images.

ArcMap was also used in the analysis of channel bar field surveys. Accurate perimeters of the channel bars were established by tracing individual points in ArcMap. Polygons produced with this method allowed for a visual as well as quantitative interpretation of change in channel bar area. Additionally, with the use of 3D analyst each point shapefile was converted to a raster. This produces a 3D visualization of points which contain X, Y and Z data. Due to the considerable amount of data points associated with the Leica Scan Station c10 baseline survey, a terrain data model was created for this particular survey from the point shapefile. This approach creates a highly accurate visualization of changes in topography across the bar surface, and allows for precise determination of volume. Similar to the previously described surveying method, points in the baseline survey were traced to produce a channel bar polygon which could be directly overlain on either an historic aerial photograph or subsequent surveys to observe changes in bar morphology.

CHAPTER 5: RESULTS AND DISCUSSION

Historic Flow Conditions

Channel bar development is largely controlled by stream capacity, velocity and the availability of sediment during high discharges. Bars therefore represent key observational features for understanding the dynamics of alluvial channels (Smith, 2007). Entrainment and transportation of sediment is determined largely by stream power (Equation 4) which is defined as,

$$\omega = \gamma QS$$

where γ is the specific weight of water, Q is discharge and S is slope. Stream power also describes the erosional capability of a river.

Historic variability and trends in Q may be described with the use of a flow duration curve. For the study site, a pre- and post-impoundment curve was established. (Figure 12). The introduction of the dam at Lake Granbury caused the mid-range flow conditions or discharges in the 40% to 60% exceedance probability range to decrease. Pre impoundment flow were $39 \text{ m}^3 \text{ s}^{-1}$ and $32 \text{ m}^3 \text{ s}^{-1}$ respectively across this range, whereas post impoundment rates declined to $9.3 \text{ m}^3 \text{ s}^{-1}$ and $1.8 \text{ m}^3 \text{ s}^{-1}$. Median flow (i.e. the 50% exceedance probability) equaled $12.8 \text{ m}^3 \text{ s}^{-1}$ before the construction of the dam, and $4.3 \text{ m}^3 \text{ s}^{-1}$ for the post impoundment period. This equals a lowering of the median flow by $8.5 \text{ m}^3 \text{ s}^{-1}$, or 34%. Before the construction of De Cordova Bend Dam, flow exceeded $20 \text{ m}^3 \text{ s}^{-1}$ 38% of the time. Under post impoundment conditions the same flow is only exceeded 24% of the time. Similarly, flow conditions exceeding $10 \text{ m}^3 \text{ s}^{-1}$ occurred 54% of the time pre-dam construction versus 39% post-dam. It would be expected that the construction of the dam increases low flow ranges as peak discharges are dampened or

eliminated. However, the flow duration curve for this section of the Brazos suggests that even after the construction of the dam, low flow conditions had a lower occurrence frequency compared to pre dam conditions. This trend is most likely the result of increasing water allocation demands from surrounding cities with growing populations. The introduction of the dam into the river system produced an overall lowering of median discharge rates. As transportation and entrainment of sediment is directly related to discharge, it may be suggested that by lowering Q , and therefore ω , the river's ability to transport material decreases.

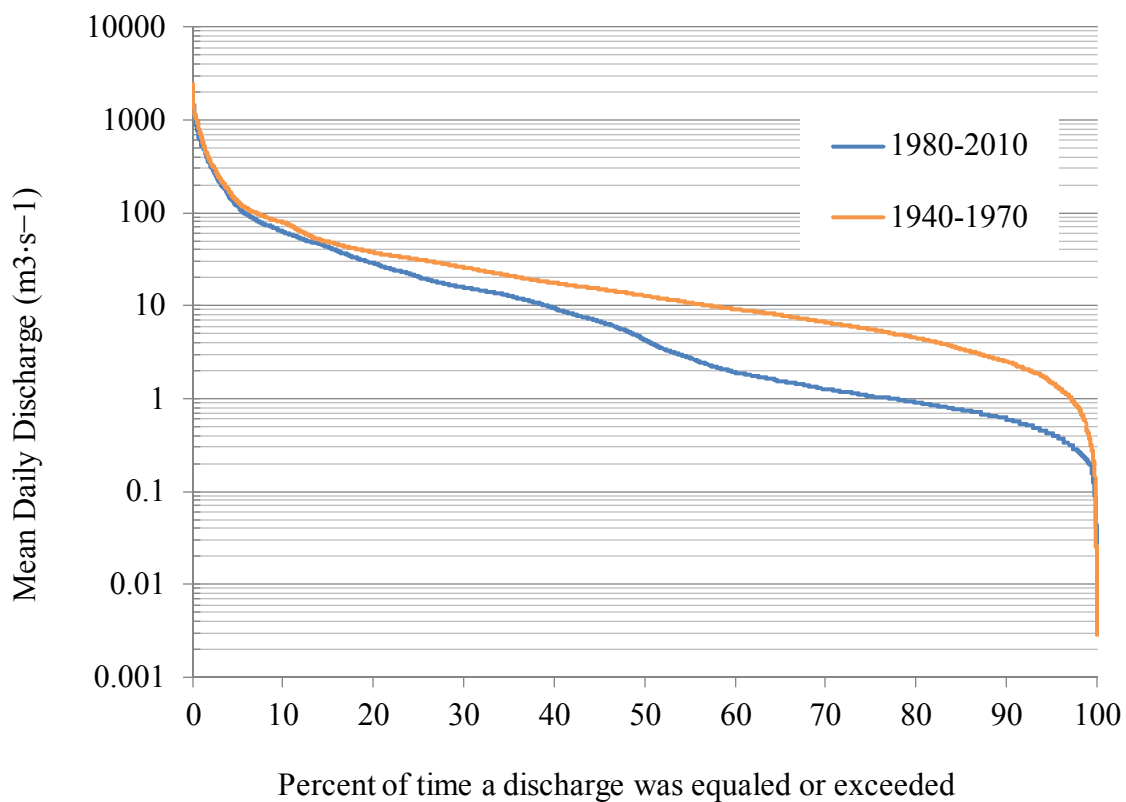


Figure 12. Flow duration curves showing flow trends before and after construction of the dam

Analysis of historic photography

To understand historic channel bar morphology, the obtained aerial photographs were digitized to allow for visual analysis. The channel bars along the study reach were divided into bar 1-A, 1-B, and 1-C (Figure 13). Each of the individual channel bars was analyzed for areal change. Directly comparing the extent of the bars between 1949 to 1984, suggests that even though bar area may have fluctuated the overall location of the channel bars in the study reach as well as river channel have remained relatively stable (Figure 14). It is important to note, however, that flow levels vary between each photograph and therefore the degree to which the bar is inundated or exposed varied. For example, the earliest photograph dating to 1949, was taken on March 9th when the mean daily Q equaled $4.53 \text{ m}^3\text{s}^{-1}$ which corresponds to a contemporary gage height of 1.62 m. The data from USGS gaging station 08091000 suggest that the photograph taken in 1959, on Feb. 6th, shows a mean daily Q of $6.63 \text{ m}^3\text{s}^{-1}$ which currently would produce a gage height of 1.64 m. This produces a difference of 0.02 m in gage height between the two photographs.

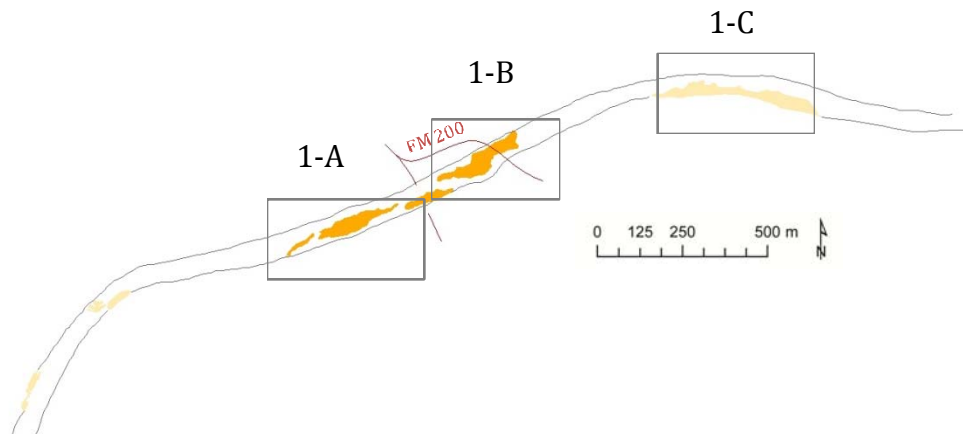


Figure 13. Locations of individual channel bar complexes along study reach

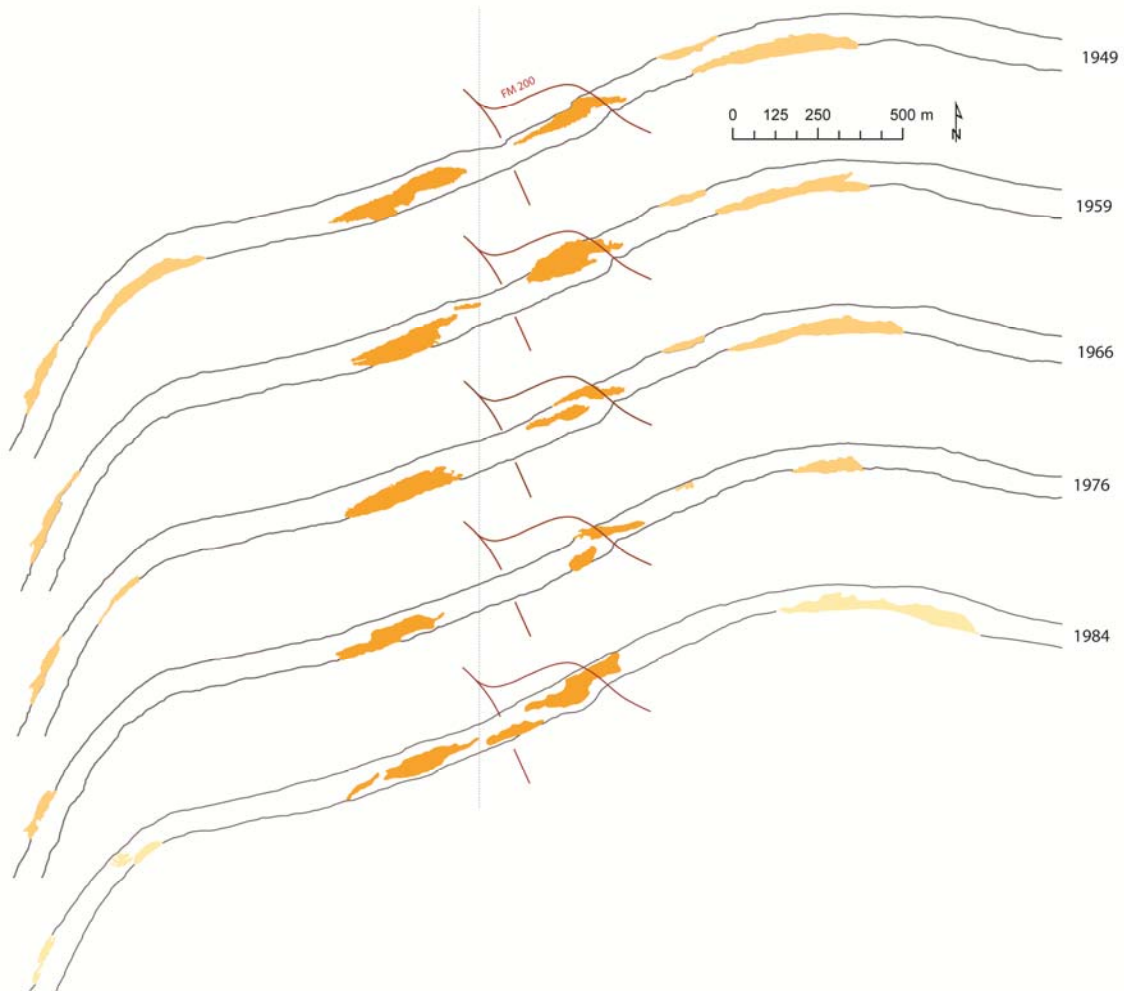


Figure 14. Visual comparison of channel configuration and bar locations established from historic photography (1949 to 1984)

Visually the areal extent of the 1949 downstream channel bar appears larger than the 1959 channel bar; however, this is most likely due to a greater degree of inundation in latter year. Digitization in ArcGIS of channel bars allowed for the precise calculation of the areal extent from year to year. In order to take into account the varying gage heights, an inundation curve was established (Figure 15). Endpoints of the curve were determined through contemporary observations of bar inundation at varying flow levels. As the study period for this project extended from February 2011 to March 2012, a range of different flow levels were observed and documented. Lowest flow levels observed at $0.45 \text{ m}^3\text{s}^{-1}$

correspond to a gage height of 1.45 m. These conditions exposed the entire downstream channel bar. Discharge rates under which the entire bar was inundated equaled $32.85 \text{ m}^3 \text{ s}^{-1}$ with a gage height of 2.14 m. This suggests that it requires an increase of gage height equivalent to 0.69 m to completely inundate the downstream portion of the channel bar. Knowing the two endpoints, an inundation curve shown in figure 14 was established where a gage height of 1.45m corresponds to 0% inundation and 2.14m corresponds to 100% inundation. As all obtained photographs were received with metadata including accurate information of date and time when the image was taken, the necessary USGS flow data could be obtained. Each year was then placed on the inundation curve according to the specific flow conditions shown in each image. Even though the gaging station has a long-term record for Q, dating back to 1923, the same is not true for gage height. The stage data record for the study area commences in 1988 and therefore a stage-discharge relationship can only be established between 1988 to the present. Comparing stage-discharge between 1992 and 2000, and 2000 to 2008 suggest only a slight shift in the relationship over a 16 year period. However, it is uncertain if the relationship will hold true over a multiple decadal time scale. Matching contemporary stage measurements with historic discharge events may introduce a degree of error in the determination of bar inundation rates.

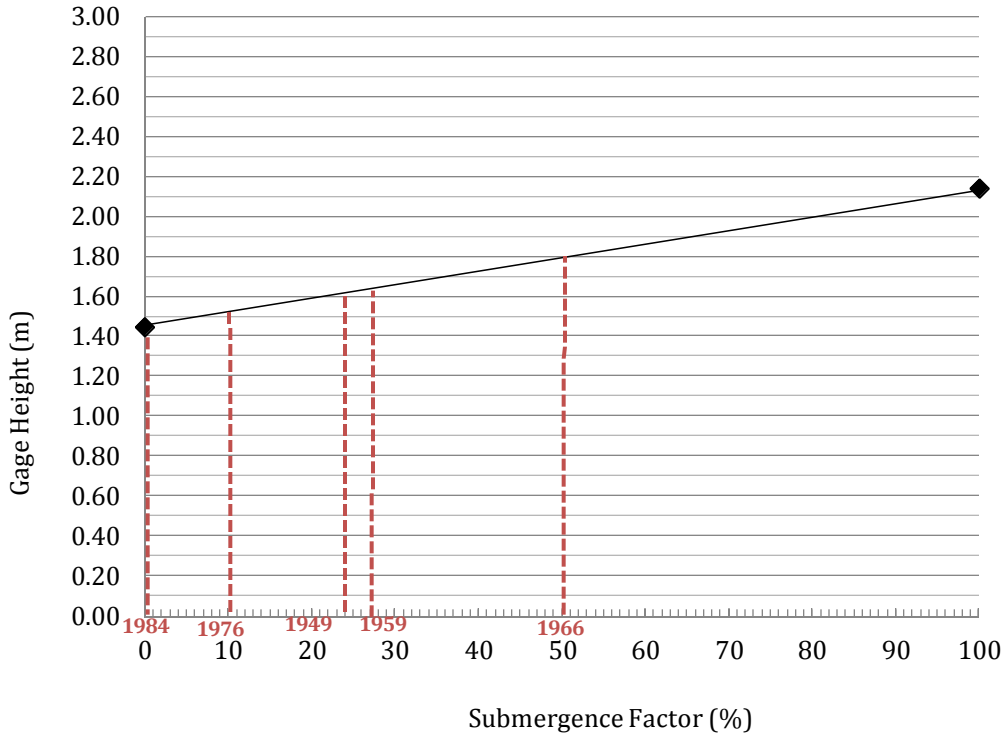


Figure 15. Inundation curve used to establish corrected channel bar areas

Channel bar 1-A is located downstream of the FM 200 Bridge. This bar complex corresponds to the contemporary channel bar surveyed over the study period. Therefore results from historic imagery can be used to determine change from 1949 to 2012. Due to time constraints channel bar surveys were not completed for bars 1-B or 1-C. Table 1

Table 1. Revised area calculations for channel bar 1-A. Calculations may be compared with contemporary field surveys

Year	Bar 1-A (m ²)	Gage Height (m)	% inundated	Inundated Area (m ²)	Revised Bar 1-A Area (m ²)
1949	18,769	1.62	24.5	4,598	23,367
1959	16,858	1.64	27	4,552	21,410
1966	17,170	1.80	50	8,585	25,755
1976	13,573	1.52	10	1,357	14,930
1984	18,647	1.45	0	0	18,647

shows that inundation rates fluctuated between zero to 50% and therefore inundated areas between photographs varied significantly. The revised bar areas show that channel bar 1-A remained relatively stable from 1949 to 1966, during the period marking pre-construction of the dam. A decline in area of 9% is observed between 1949 to 1959, and an increase in area of 17% from 1959 to 1966. Post-dam construction imagery taken in 1976 shows a more significant shift in area. A comparison between 1966 and 1976 suggest a decline in area of 43%. The observed shift may be directly attributable to the interruption of sediment transport due to the construction of the dam. In essence, decreasing the sediment supply alters the natural equilibrium. The equilibrium equation (Equation 2) states that for any geomorphic system a change in storage is explained by the difference between the input and the output. For the case of the study reach it appears that with the introduction of an impoundment erosive forces removed more material than were replenished therefore producing a net decrease in storage.

Numerous studies have shown that large amounts of sediment may become trapped behind a dam structure producing sediment starved waters downstream (Graf, 1999; Kondolf, 1997). This initial imbalance in sediment supply may result in increased scouring of downstream reaches as the river attempts to readjust its sediment load. Even though the natural sediment delivery ratio is altered by the construction of an impoundment, large amounts of sediment can still become mobilized due to the increased erosive force of the water released downstream. An increase of sediment supply due to prolonged scouring may be responsible for the observed overall channel bar growth in the 1984 historic photograph, and change observed in bar 1-C.

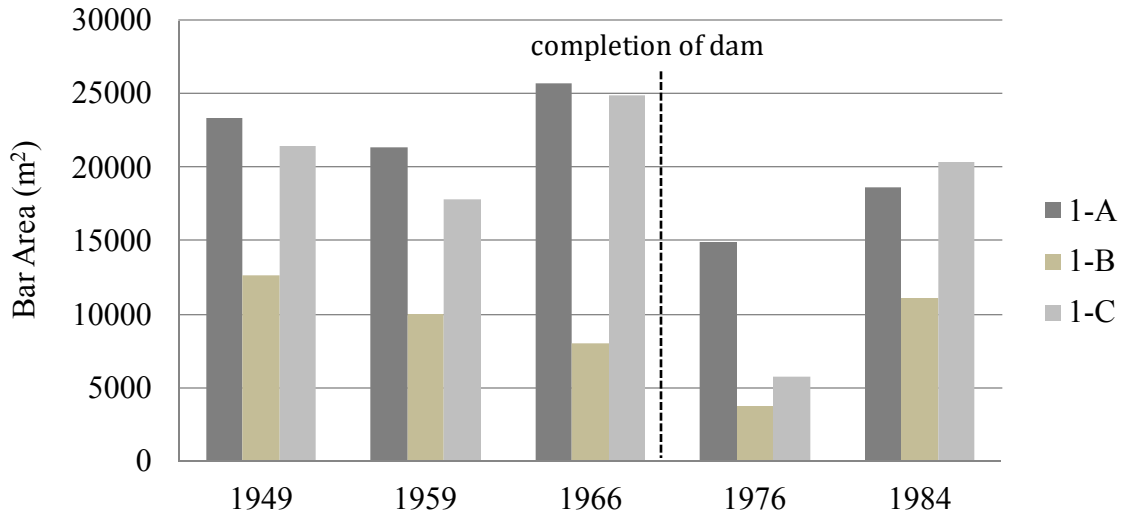


Figure 16. Comparison of channel bar area across the reach for each of the historic images

Similar trends are observed for channel bar 1-B and 1-C in the upstream reaches of the study site (Figure 16). A stable channel bar is calculated for the pre-construction period from 1949 to 1966 with a sharp decline in bar area post-construction for both 1-B and 1-C. Channel bar 1-B shows a reduction in bar area of 54%, whereas channel bar 1-C declined by 77%. All three channel bar complexes show an areal increase in 1984. Changes in bar morphology are directly related to the available stream power. It is therefore necessary to compare storage changes to observed annual flow trends (Figure 17). In the comparison of 1949 and 1959, a decline of bar area is observed in the entire reach. When combining this trend with specific annual discharge over the same time frame, it becomes evident that a significant discharge event in 1957 could be responsible for the shift. In May of 1957 discharge rates reached a maximum of $2400 \text{ m}^3 \text{ s}^{-1}$, with elevated flow levels sustained for most of the month. As this period marks a pre-impoundment channel, flow was not regulated and therefore peak flows attained. A significant increase in discharge will raise stream power and the river's ability to flush

stored sediments. A second trend observed between the three channel bar complexes is a steady growth from 1976 to 1984 (Figure 17). This increase in bar area follows the sharp decline observed in the initial post impoundment phase. It might be suggested that an initial reduction in sediment load is responsible for the decline observed in 1976. The growth in 1984 can be explained by either increased sediment mobilization due to scouring below the dam or by variations in climatic conditions. A comparison with the annual discharge trends shows a second significant flow event occurred in 1982. In June of 1982, maximum flow levels were recorded at $1280 \text{ m}^3 \text{ s}^{-1}$, with elevated discharges recorded mid-May through early July. Prolonged precipitation and erosion can significantly increase sediment supply in the reach below the dam. As flow was regulated during this period it is unlikely that natural peak flows were attained. Flow regulation alters the natural hydrograph of a river by potentially increasing the slope of the rising limb while extending the length of the recession limb. Sediment deposition occurs along the recession limb as flow slows down and material can no longer be held in suspension or transported along the bed.

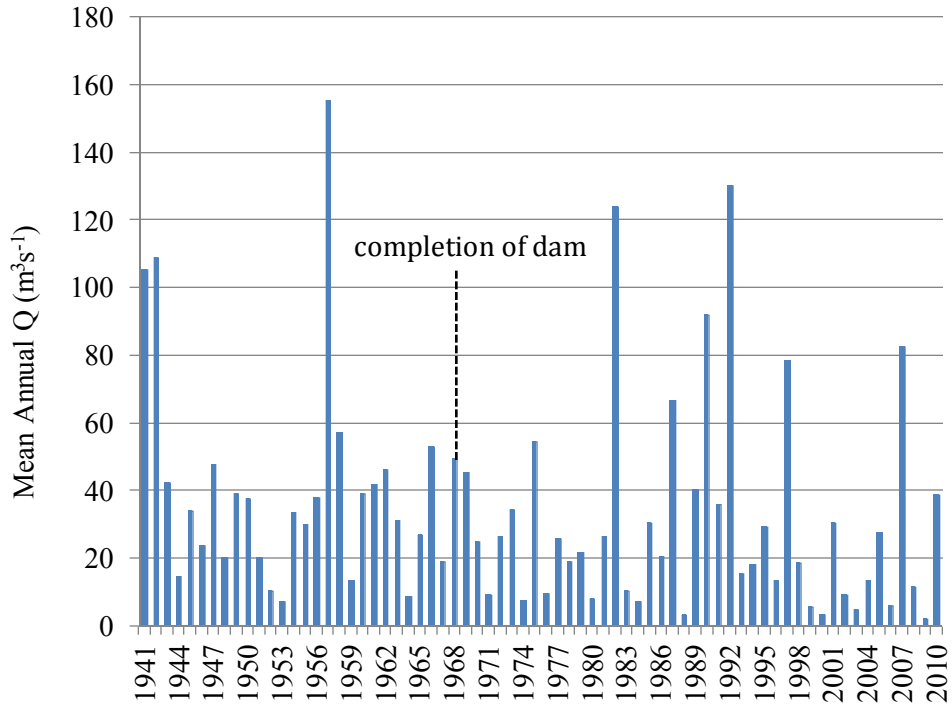


Figure 17. Fluctuations in mean annual discharge rates at the study site 1941 to 2010

In order to determine the validity of the assumption of increased sediment mobilization below the dam, two additional aerial photographs were obtained showing the exact location of De Cordova Bend Dam in 1958 and 1976 (Figure 18). A significantly scoured region was observed below the dam in 1976, with an areal extent calculated to 2,448 m². An additional comparison to a 2010 photograph suggests continued scouring, increasing the affected area to 3,784 m². However, in addition to bank erosion and scour there is also evidence of bar formation in 1976. A substantial bar complex was measured to comprise 2,851 m². There is no evidence of the same bar formation in 1958.

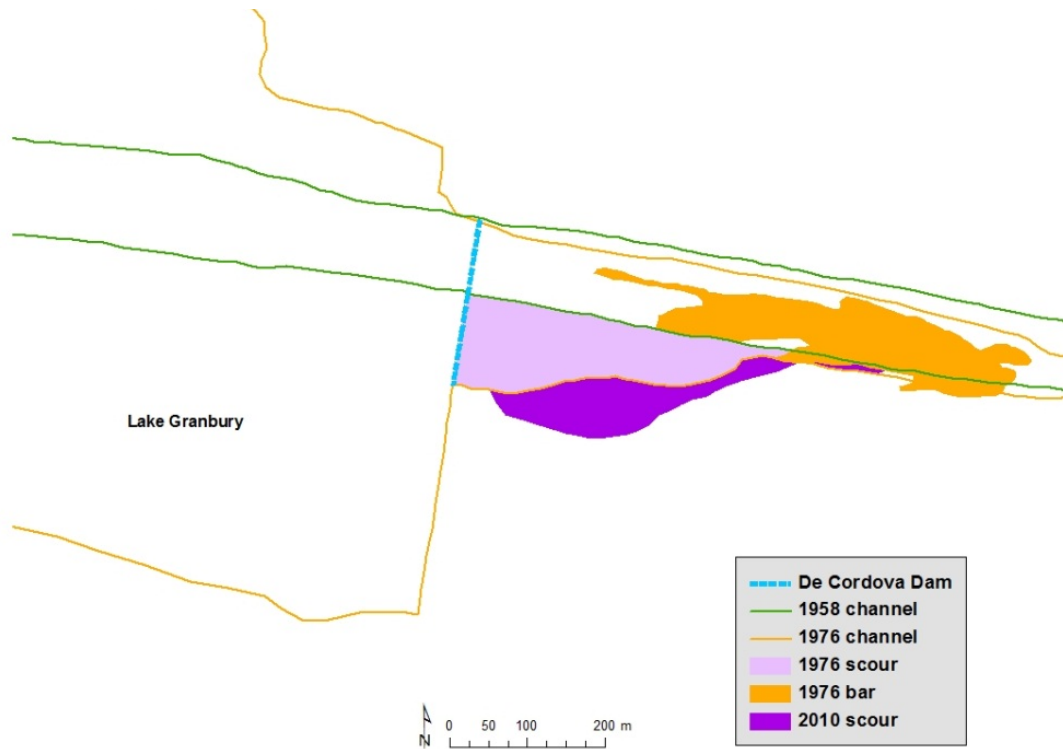


Figure 18. Channel scour for post construction years observed through photographic analysis

Material removed below the dam due to channel scour appears to be deposited directly downstream rather than mobilized and transported over a longer distance. Philips (2005) suggests that effects of “hungry water” below an impoundment are often localized, however, effects of flow obstructions and subsequent changes in downstream hydraulics may be manifested by fluctuations in width, depth and slope of the channel along specific cross-sections. Additionally, it should be noted that downstream effects of a river impoundment can become masked by specific climatic conditions experienced during the post construction period. Between 1969 and 1976 no significant discharge events were observed. Mean annual Q varied between $8 \text{ m}^3\text{s}^{-1}$ and $55 \text{ m}^3\text{s}^{-1}$. The absence of a high annual discharge over the seven-year period suggests that the decrease in bar area observed in 1976 may in part be due to a prolonged period of decreased discharge

rates reducing material availability. To date, the exact upstream region responsible for sediment supply to the channel bars has not been determined. Additional photography may be obtained to further examine trends of erosion and deposition in the 40 km reach between the study area and Lake Granbury.

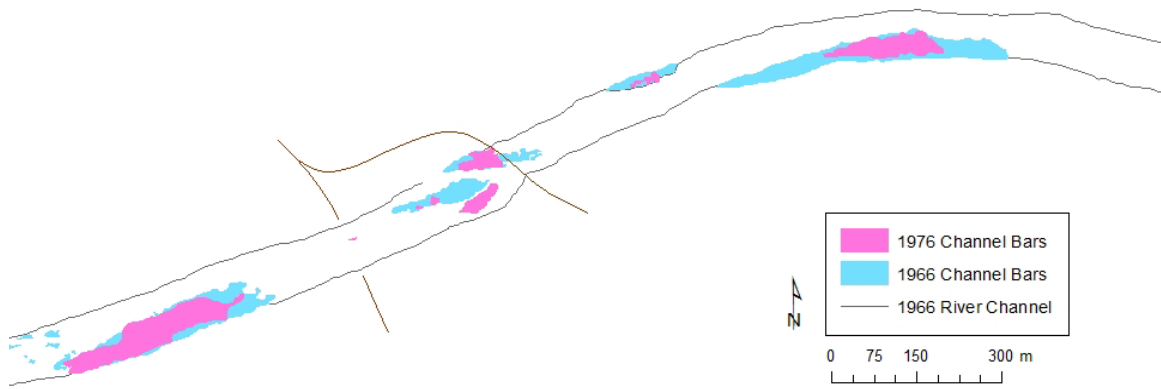


Figure 19. Comparison between channel bar locations 1966 to 1976

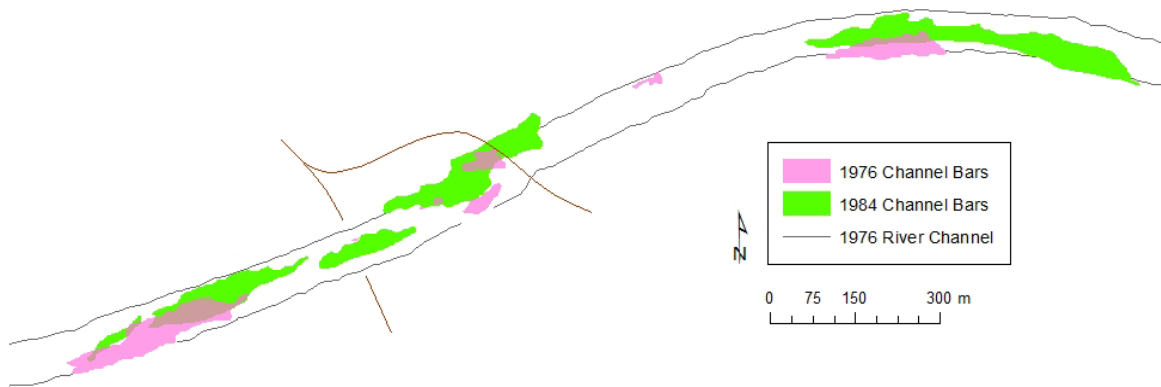


Figure 20. Comparison between channel bar locations 1976 to 1984

Channel Bar Surveys

2011 marked a year of extreme drought for large parts of Texas. The state experienced a combination of record setting temperatures and low precipitation rates. Discharge levels in the Brazos were reduced and sustained for much of the summer and fall. With low precipitation rates during these months, gage height fluctuated between 1.50 m to 1.75 m (Figure 21). Successive patterns in rising and falling stage from May 2011 to December 2011 marks periods of controlled dam release. Due to extensive drought conditions, the Brazos River Authority continuously released water from Lake Granbury to relief shortages in downstream reaches. The single substantial increase in discharge and stage was observed during late January 2012 when the area received nearly 11 cm of rainfall over a 48-hour interval. In order to establish short-term change in morphology, channel bars were repeatedly surveyed. The initial plan included an extensive survey to be completed every two months throughout the study period. However, due to the lack of variation in flow conditions surveys were obtained March 2011, April 2011, October 2011, and March 2012.

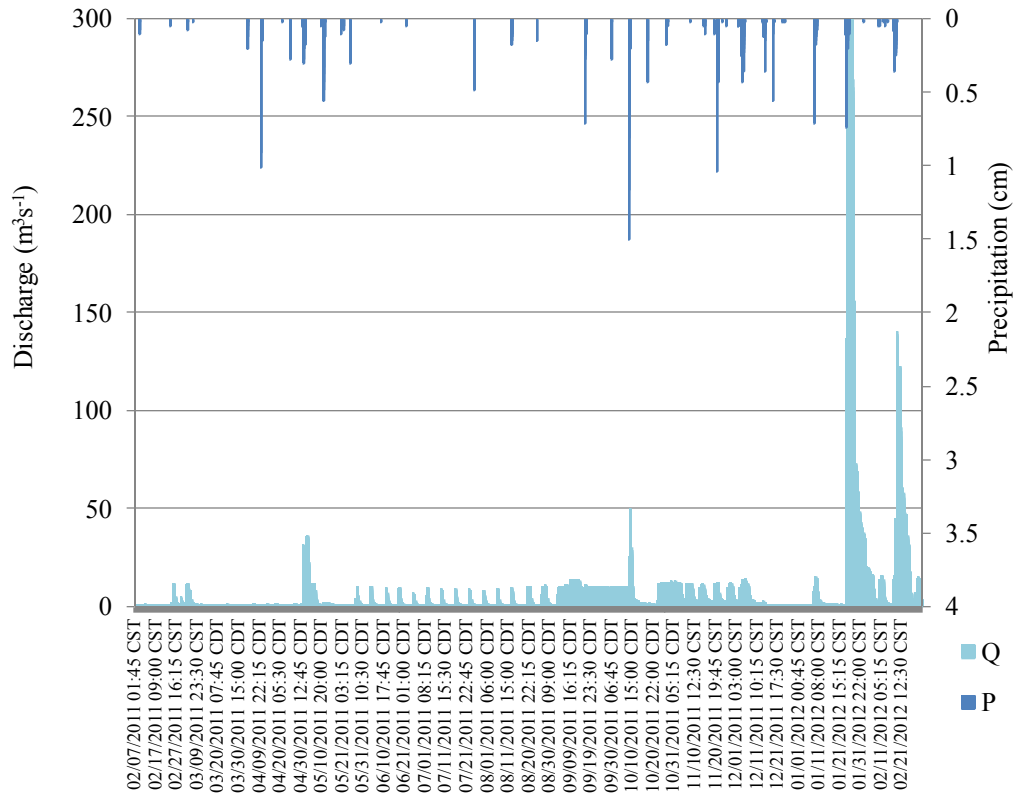


Figure 21. Discharge trends for February 2011 to March 2012 compared with rates of precipitation

The first baseline survey was completed on March 12, 2011 at a gage height of 1.50 m with the use of a Leica TS02 Flexline Total Station. This survey measured total bar area to 20,504 m². A second survey was completed on April 1st, 2011 using a Leica Scan Station c10 at a gage height of 1.51 m. It must be noted that all subsequent surveys used the Leica TS02 Flexline Total Station. The two surveying methods show a significant difference in capacity. The scan station utilizes a laser beam capturing point cloud data through which it can establish the exact location of the wetted perimeter. The Flexline total station method requires the manual operation of a reflector while walking the perimeter of the channel bar. This method therefore captures significantly fewer points and has a greater potential for human error and inconsistency. Measurements

obtained during the April 2011 baseline survey suggest a planform area of 19,360 m² and a volume of 22,928 Mg at a plane height of 171.73m. This survey allowed for the accurate determination of variation in topography across the channel bar, establishing that the range in elevation varies between 172.83 m to 172.28 m. A terrain data model established with the survey data suggests that bar accretion occurs laterally towards the mid sections of the bar, and lowest elevations are found in the lower bar reaches (Figure 22).

As with the photography time series analysis, specific flow conditions must be taken into account when comparing between surveys. With the use of the same inundation curve it was established during the April 2011 survey that 9.6% of the channel bar was inundated and therefore the actual bar area exceeded what was measured during the survey. The revised channel bar area equaled 21,219 m². Subsequently, the second survey completed in October 2011 was obtained at a gage height of 1.45m. According to observations made over the duration of the study period, this gage height marks a 0% inundation rate. Therefore, the area obtained during the survey did not have to be adjusted to include inundated sections. For this survey, planform area measured 22,142 m². This suggests a slight increase in bar area of 924 m² between April and October 2011. The apparent change may be explained by reduced stream power due to low flow conditions, and therefore the reduced ability to transport material downstream. Some evidence of scouring is visible at the upstream portion of the bar (Figure 23). This area is considered the bar head and is subjected to flows of highest velocity and erosive capability. Extreme downstream portions of the bar appear to show increased deposition. Again, it must be taken into consideration that surveys were completed under varying

flow conditions and therefore GIS representations show uncorrected planform areas. The significant difference

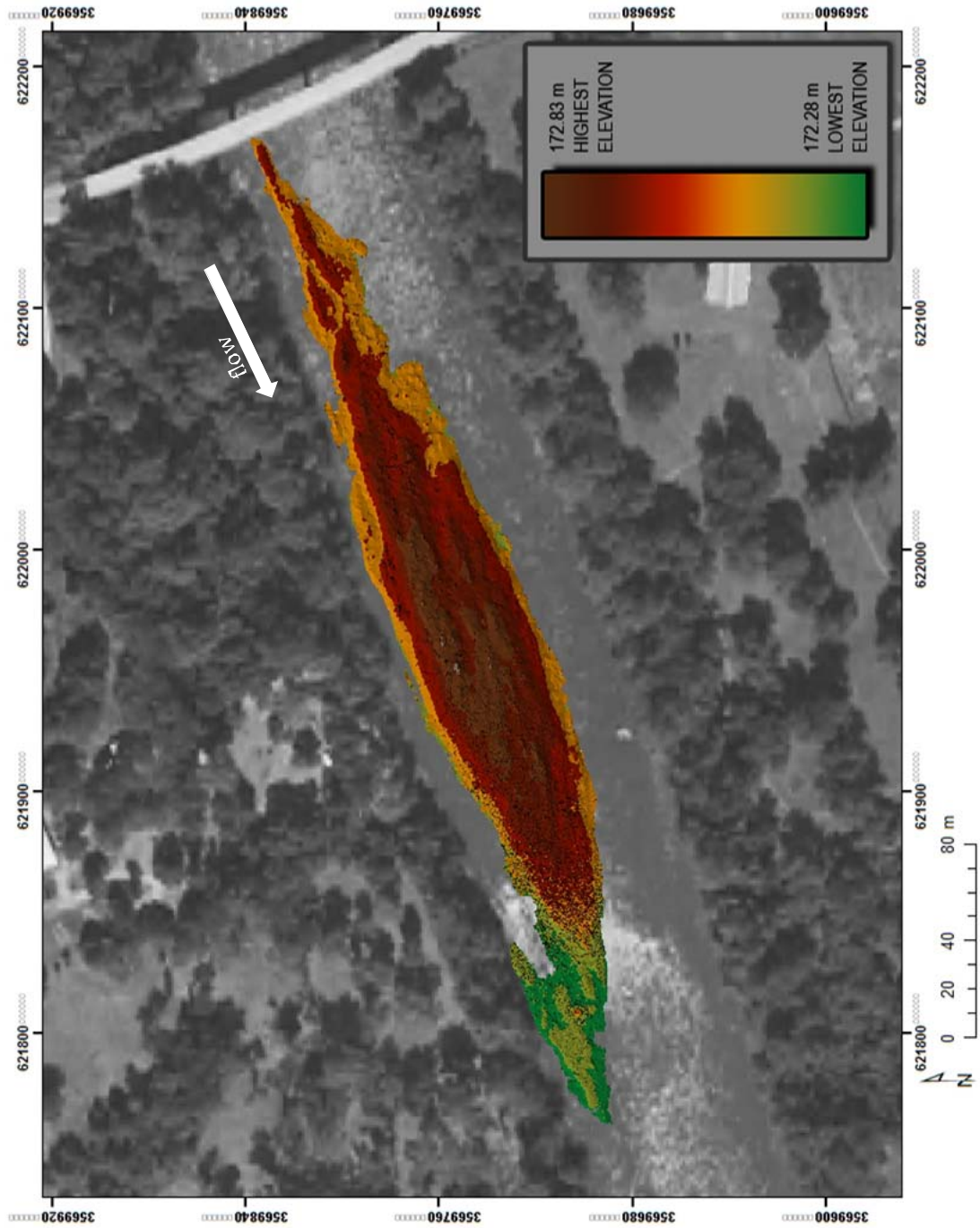


Figure 22. April 2011 Terrain data model showing range of elevation across the mid channel bar

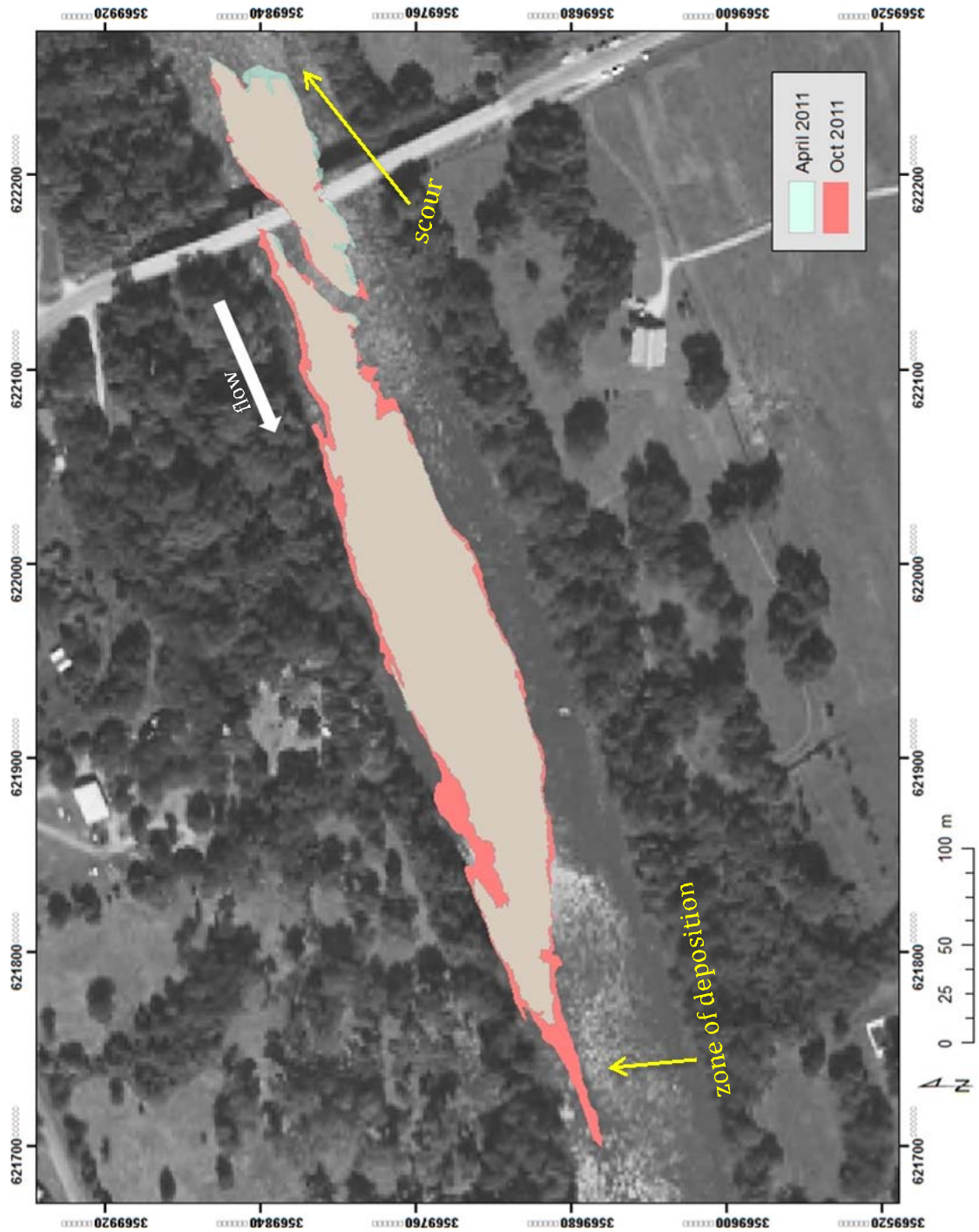


Figure 23. Overlay of April 2011 and October 2011 surveys showing areas of scour and deposition

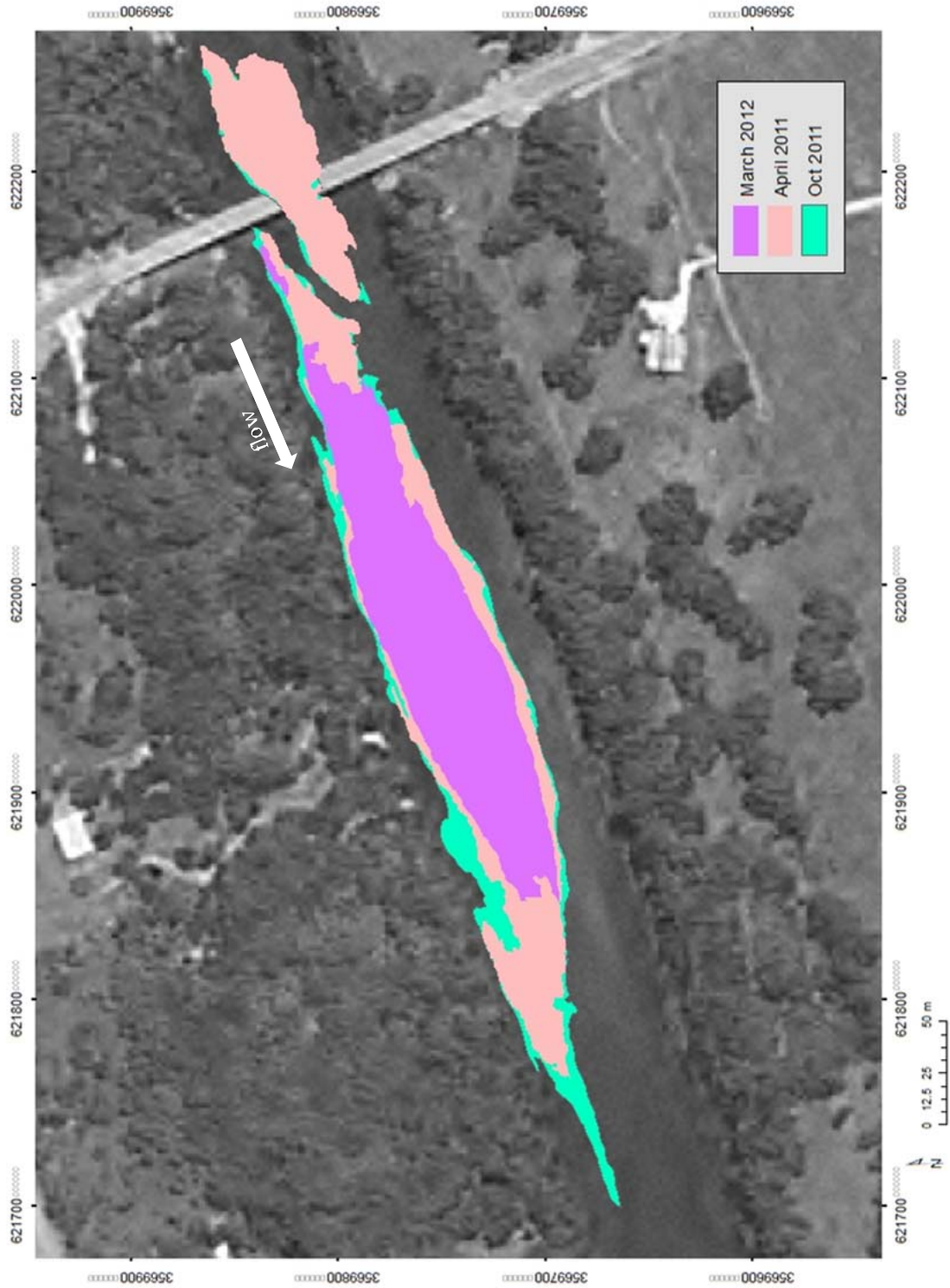


Figure 24. Overlay of completed surveys April 2011, October 2011 and March 2012

between the surveying methods used in the April and October may also lead to the apparent change in bar morphology. A comparison made between the March and April 2011 survey may help to clarify the degree of error. Mean discharge rates observed in the time between the two surveys ranged from $0.96 \text{ m}^3\text{s}^{-1}$ to $1.16 \text{ m}^3\text{s}^{-1}$ and gage height fluctuated between 1.49 m to 1.51 m. These low flow conditions should not produce a substantial change in bar morphology; however when comparing the revised bar areas there is an apparent increase in planform area of $1,013 \text{ m}^2$ (Table 2) This may suggest increased deposition due to low flow conditions, however the change is measured over a period of one month and a substantial areal change would not be expected to occur within this time frame. To reduce error, a direct comparison should be made between the March 2011 and October 2011 surveys which both utilized the Leica TS02 Flexline Total Station. These surveys suggest an increase in areal extent of $1,938 \text{ m}^2$.

Table 2. Planform area measurements showing original and revised calculations for the entire bar complex

Date	Surveyed Area (m²)	Gage Height (m)	% inundated	Inundated Area (m²)	Revised Total Bar Area (m²)
03/2011	18,709	1.50	8	1,497	20,205
04/2011	19,360	1.51	9.6	1,859	21,219
10/2011	22,143	1.45	0	0.0	22,143

Table 3. Revised planform area calculations separating upper and lower portions of the channel bar

Date	Upper Bar Area (m²)	Δ Area (m²)	Lower Bar Area (m²)	Δ Area (m²)
03/2011	3,650		16,554	
04/2011	4,010	360	17,206	652
10/2011	3,459	-551	18,684	1,478
03/2012	n/a	n/a	12,637	6,047

When comparing between surveys, the trends in upper and lower bar area change should be considered separately (Table 3). Most noticeable, between April 2011 and October 2011 there is an overall increase in bar area of 924 m². However, when separating planform area change between the upper and lower portion of the bar it becomes evident that there is an unequal distribution of change across the entire bar. The upper portion actually experienced a decrease in planform area of approximately 551 m² whereas the lower portion experienced most of the growth with an estimated increase of 1,478 m². This supports the assertion that upstream portions of the channel bar are exposed to higher erosive flow conditions under which material is easily removed which is subsequently deposited in the lower reaches of the bar.

A fourth and final survey was completed on March 4th 2012 at a discharge of 3.25 m³s⁻¹ and gage height of 1.59 m (Figure 24). Ideally, the survey would have shown channel bar extent over low flow conditions. Due to infrequency of these events during spring months this was not attainable. The entire channel bar area could not be surveyed as higher inundation rates covered upstream portions of the bar. With the use of the inundation curve, planform areal measurements obtained during this survey were revised to suggest a significant decrease in bar area of 6,047 m² from October 2011 to March 2012 (Table 4). This establishes a decrease of approximately 33%. A substantial storm event experienced in late January 2011 is most likely responsible for the majority of this change. High discharge rates for this event exceeded a 1991 record and greatly increased stream power, therefore increasing sediment entrainment and transport.

Table 4. Planform area measurements for lower channel bar to include March 2012 survey

Date	Surveyed Area (m ²)	Gage Height (m)	% inundated	Inundated Area (m ²)	Revised lower Bar Area (m ²)
03/2011	15328	1.50	8	1226	16554
04/2011	15700	1.51	9.6	1507	17207
10/2011	18684	1.45	0	0	18684
03/2012	10358	1.59	22	2279	12637

Interpretation of survey transects

Additionally to establishing a new channel bar perimeter, the March 2012 survey aimed at reconstructing previously determined transects across the lower portion of the bar (Figure 25). The exact location of these transects were determined with the use of a GeoXH unit. Transects were then re-walked to determine change in Z. Newly obtained elevations could be compared with October 2011 data to determine the degree of aggradation and degradation across the channel bar after a substantial storm event.

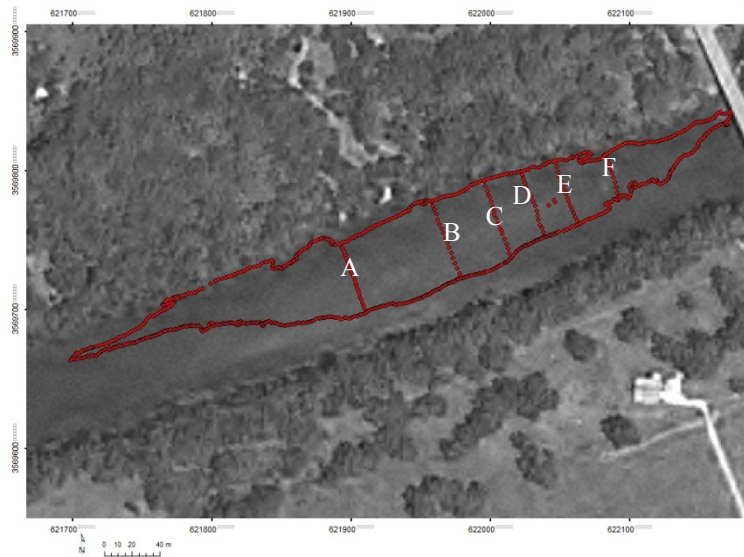
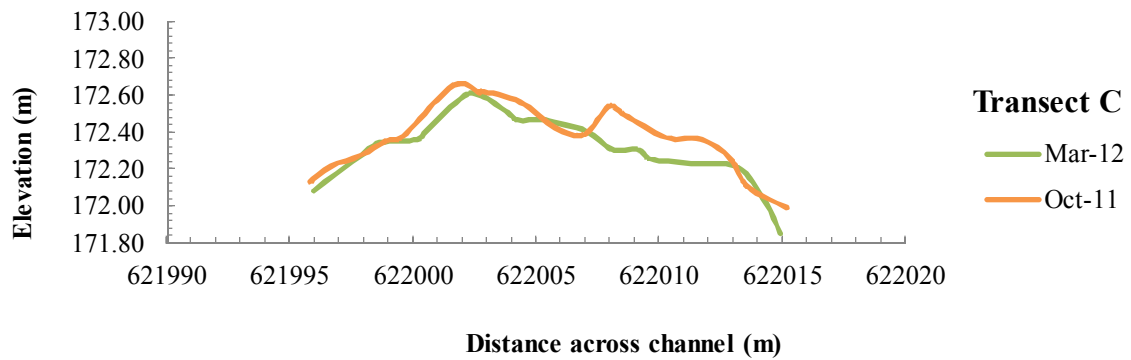
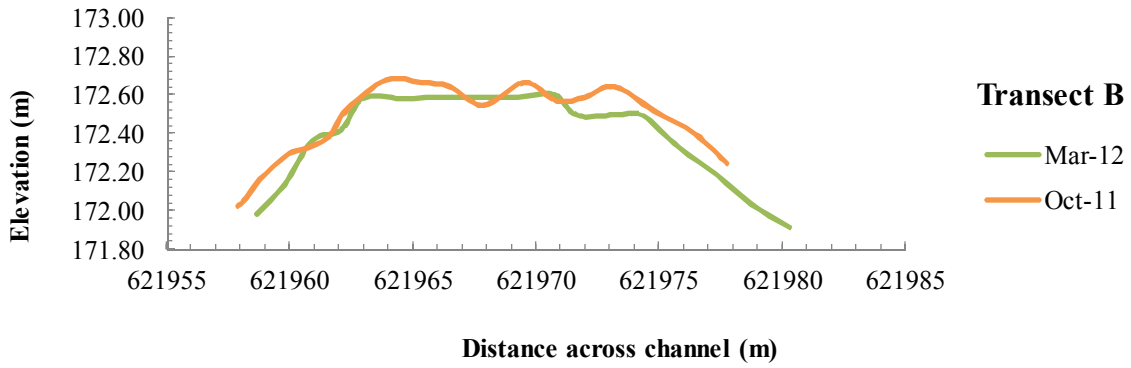
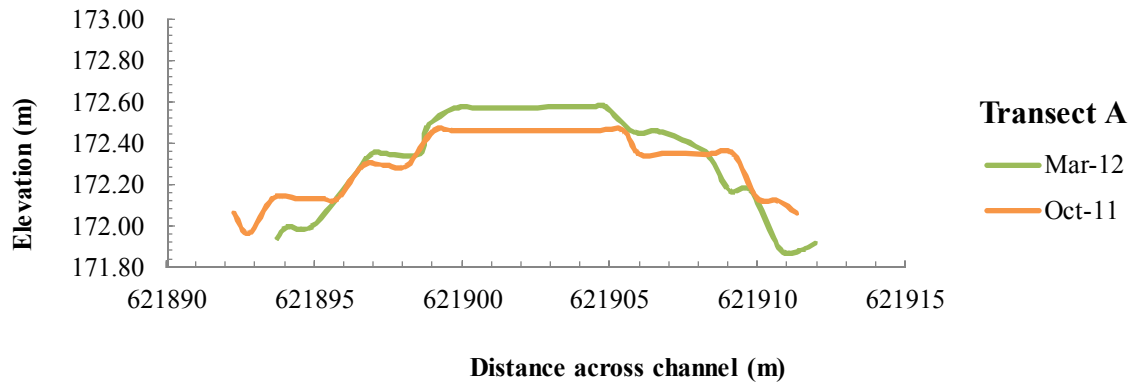


Figure 25. Location of transects for October 2011 and March 2012 surveys



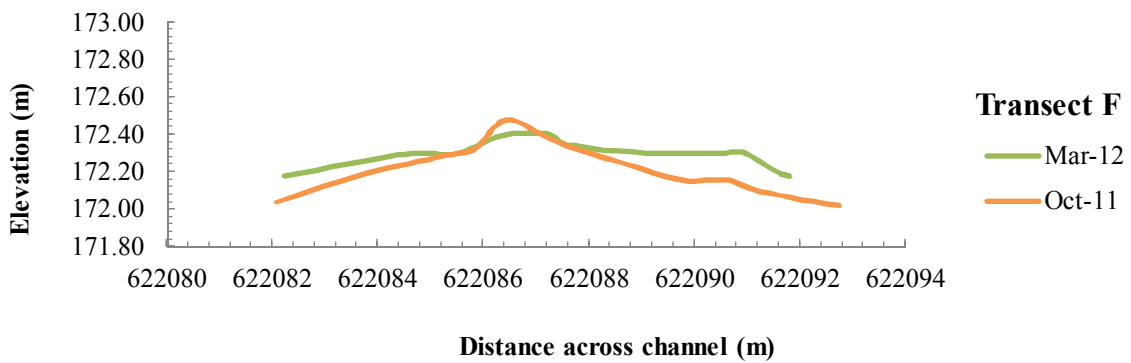
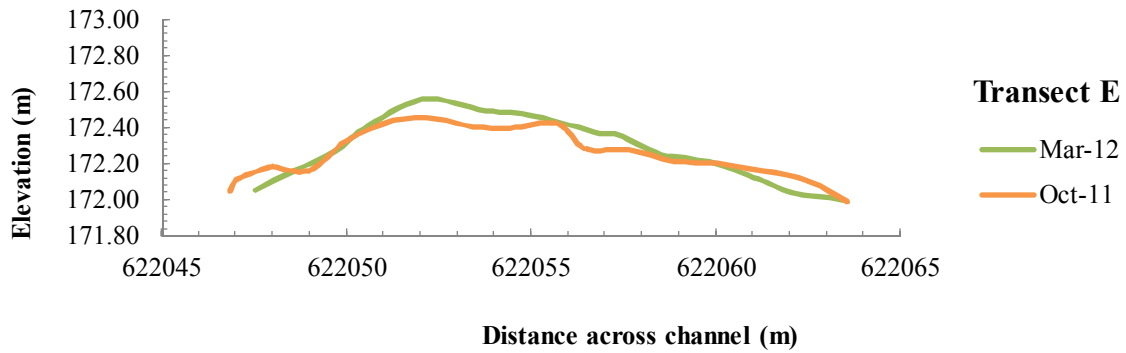
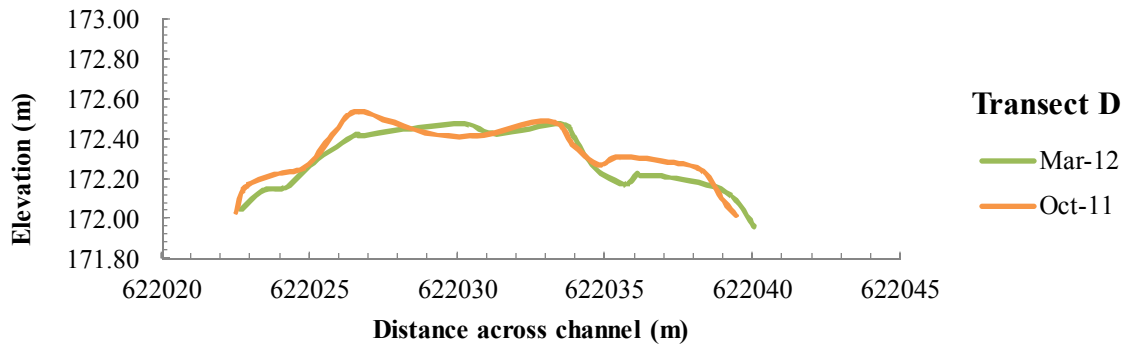


Figure 26. Comparison of 6 transects across the channel bar showing topography change from October 2011 to March 2012

Transect A, along the lowest reach of the bar, shows evidence of aggradation along the midsection and degradation along the edges and bar slopes (Figure 26). With the use of the trapezoidal method, areas below the individual transect curves were

determined and compared to determine change between October to March. Even though transect A shows areas of aggradation and degradation, a net increase in area was calculated to 0.79 m^2 along this transect. In general, a substantial storm event is expected to remove material along the edges as well as the top of the bar. Evidence of edge trimming is visible; however, aggradation along the top and midsection of the bar may be due to increased sediment deposition along the recession limb of the storm. During this period, discharge tends to decrease and therefore stream power, or the river's ability to transport material, decreases. On the recession limb, material availability may not be completely depleted and deposited material can produce substantial aggradation across the bar top.

Varying rates of degradation are observed between transect B to D, or the midsection of the bar. Degradation along transect B was calculated to 2.43 m^2 , and along transect C to 1.73 m^2 , and transect D to 0.15 m^2 . However, along the upper reaches, or along transect E and F, evidence of aggradation is observed. This area signifies the zone which is most susceptible to erosive high discharge events, as it is the initial point where flow impacts the structure and considered the bar head. Therefore, velocity is highest along these reaches of the bar and slows across the length of the bar due to shallowing water depth and increased friction. Degradation would be also expected along this part of the bar and most likely occurred during the storm event; however, with decreasing discharge rates along the recession limb and subsequent lower flow conditions may be responsible for the visible building up of the profile.

Both transect E and F show an overall aggradation between October to March. Aggradation rates for transect E were calculated to 0.81 m^2 , and transect F to 2.38 m^2 .

Therefore, highest rates of aggradation occurred at the bar head. Even though individual transects show evidence both aggradation and degradation, an overall net loss of material was determined to 0.33 m² when comparing all transects. It must be noted that chosen transects give an estimate of bar behavior, and that adding additional transects to the surveying technique may alter the net result. The storm event responsible for much of the change observed between transects occurred late January 2012 and the channel bar was not resurveyed until early March 2012. The period between the two surveys experienced moderate to low flow conditions during which available limited material may have been transported and deposited along the upper reaches of the channel bar. The results of transect comparison coincides with visual analysis of the survey TIN surfaces which suggests that aggradation occurs along the bar ridge of the bar with lowest elevations found in the far downstream portion of the bar (Figure 27).

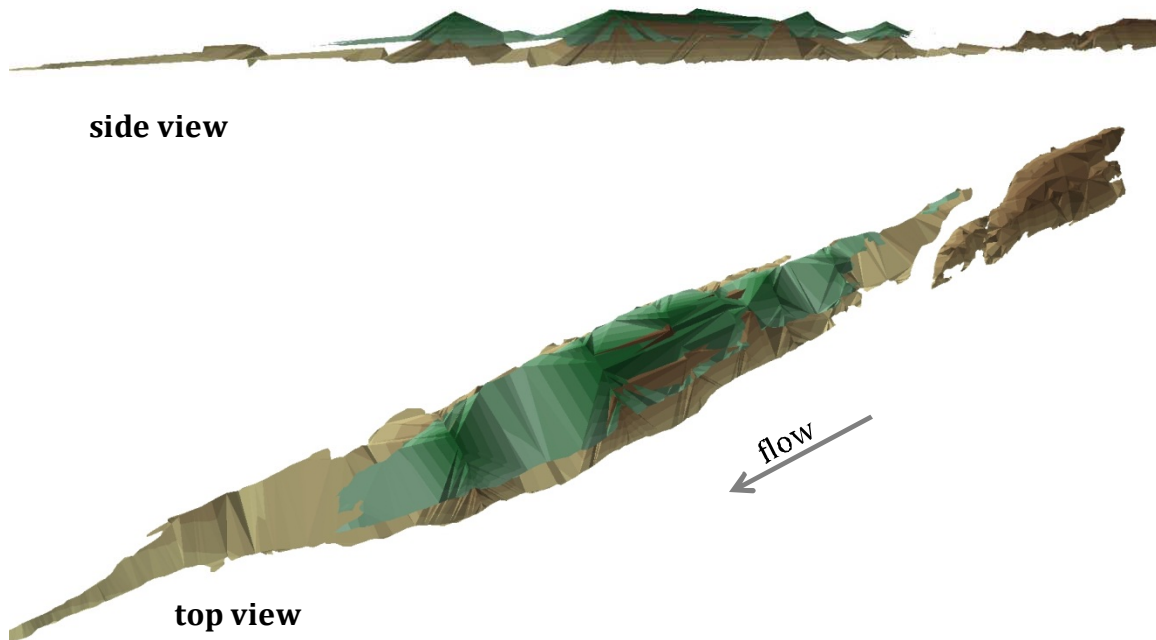


Figure 27. Overlay of March 2012 TIN (shown in green) and October 2011 TIN (shown in brown). Elevations are vertically exaggerated to show detail.

The repeated surveying technique accurately captured changes in bar morphology with seasonal fluctuation in discharge. As the study period experienced both extreme drought conditions and a high discharge event, a precise determination could be made on the short-term response in channel bar growth and decline. From the results it is concluded that substantial bar aggradation occurs over prolonged periods of lower discharge. A rapid rate of bar degradation was observed over a single storm event suggesting that channel bars are potentially highly mobile if the necessary flow conditions are in place.

Establishing a sediment record

Sediment dynamics along the study area were determined by careful sampling of suspended and bedload sediment along predetermined stations on the FM 200 bridge over a range of flow conditions. Due to drought conditions, five sample runs were completed over relatively low flow conditions. Discharge levels for these runs ranged from $2.7 \text{ m}^3\text{s}^{-1}$ to $32.2 \text{ m}^3\text{s}^{-1}$. In total, samples were obtained for three different storm events and over two scheduled dam releases. One sample run was completed over exceptionally low flow conditions to establish a baseline. The first small storm event occurred in August 2011 where peak discharge rates equaled $10 \text{ m}^3\cdot\text{s}^{-1}$ and precipitation totaled 2.39 cm over less than 24 hours (Figure 28). A hydrograph relates changes to discharge over time with rates of precipitation. For this particular storm event, a steep rising limb was observed as well as a close correlation in the peak of the hydrograph and peak precipitation rates. The steep rising limb may be due to increasing rates of precipitation with time or may be caused by a release from De Cordova Bend Dam. In order to provide flood control, lake levels in Lake Granbury are carefully monitored and water is released from the dam as needed. The hydrograph for a second storm event in October 2011 shows a more gradual rising limb and falling limb spanning nearly 24 hours (Figure 29). Peak discharge equaled $50 \text{ m}^3\text{s}^{-1}$ with precipitation totals of 14.17 cm. In the rising limb there does not appear to be evidence of a dam release. Lake levels in Lake Granbury were below average during this time of the year and therefore additional rainfall may not have exceeded desired lake levels. This suggests that the hydrograph is produced primarily by direct precipitation in the channel and by runoff added to the reach below De Cordova Bend Dam. As the above mentioned hydrographs span 24 hours or less, it was not

possible to sample over both the rising and falling limbs. Falling limb stages occurred over nighttime hours during which sampling could not be completed. The final and largest storm event was experienced late in January 2012 and created peak flow conditions allowing for sampling over $153.7 \text{ m}^3\text{s}^{-1}$ to $448.6 \text{ m}^3\text{s}^{-1}$ discharge conditions (Figure 30). Due to the longer duration of this storm event, samples from both the rising and falling limbs were included.

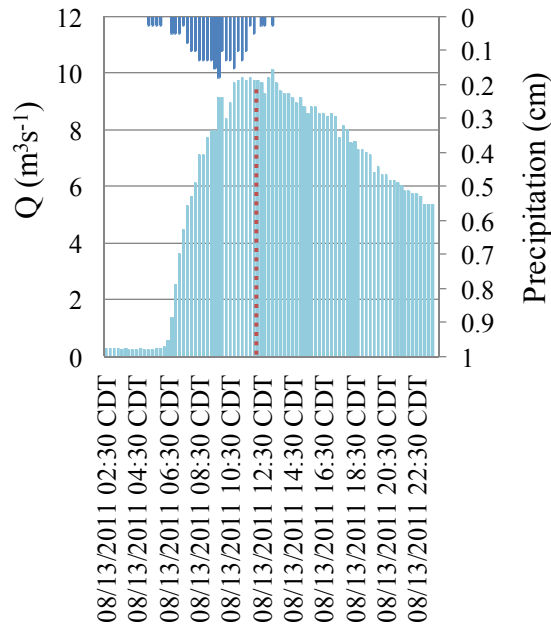


Figure 28. August 2011 hydrograph showing the relationship between discharge and precipitation. Sediment sampling time is marked by dashed line

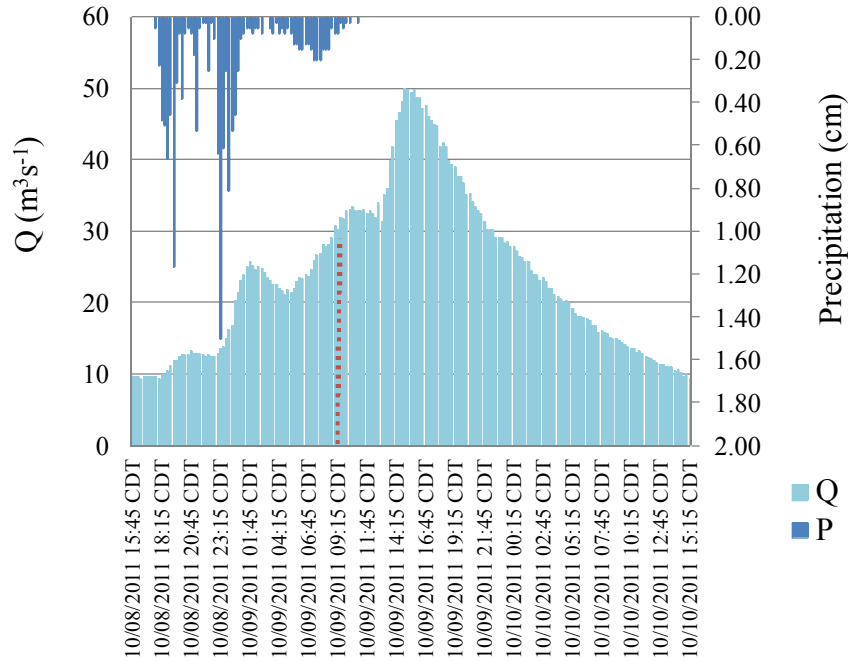


Figure 29. October 2011 hydrograph, sampling time is marked by dashed line

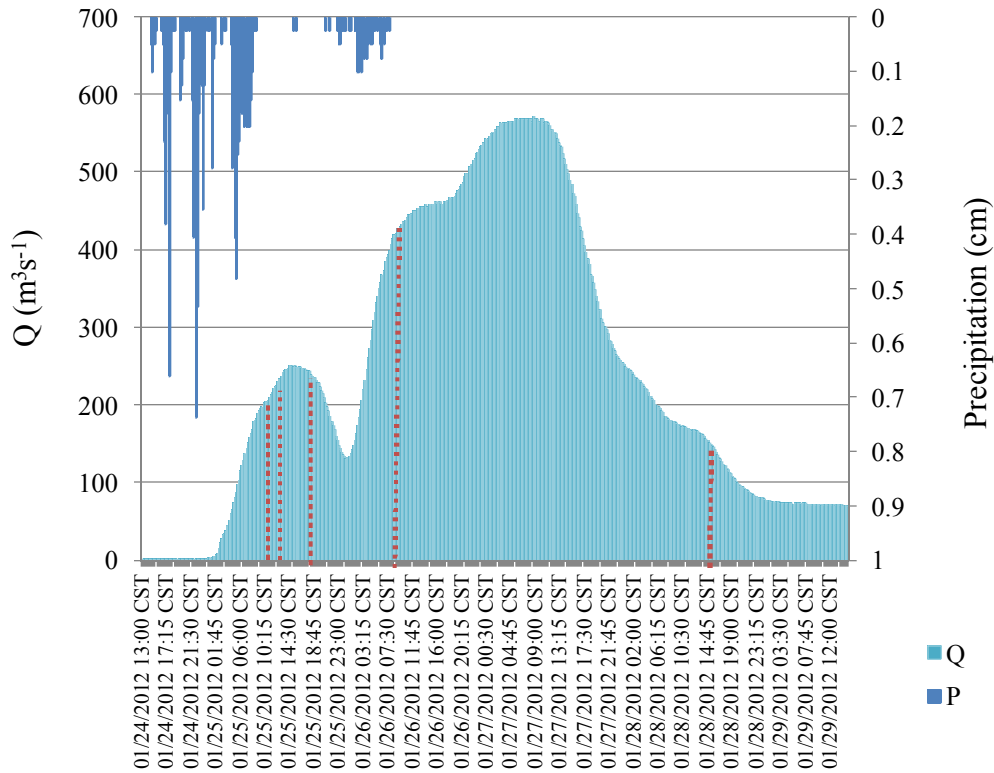


Figure 30. January 2012 hydrograph showing sediment sampling times with dashed lines

For each of the different discharge events, five samples were taken across the bridge to capture all variability in sediment flux with depth across the channel. Highest SSC values, or mass per known volume of water, were observed along stations 3 and 4. These stations coincide with areas of shallow flow depths. The mean of each sample run was taken to establish a relationship between suspended sediment concentration and discharge. Linear regression of this relationship showed an R^2 value of 0.46. The suspended sediment-discharge relationship shown in figure 31 is impacted by two sets of samples taken during the recession limb of the January 2012 storm. This

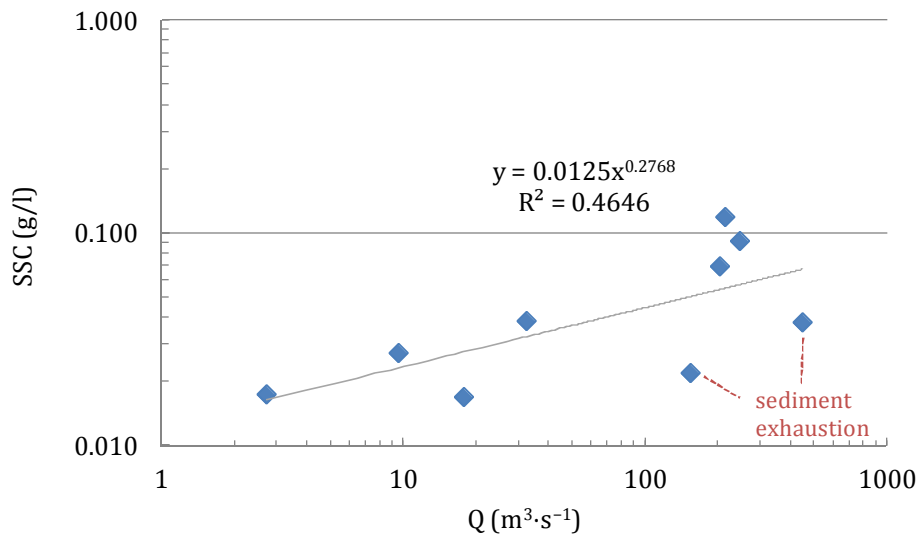


Figure 31. Correlation of suspended sediment concentration and discharge

segment of the storm event shows high discharge rates, $>240 \text{ m}^3 \cdot \text{s}^{-1}$, but relatively low suspended sediment discharge. A significant storm event will produce an increase in discharge and therefore cause an increase in turbulence. The effect of rising turbulence allows for materials to be lifted from the bed or banks of the river into suspension. Even

though discharge and turbulence remains high over the course of a storm event, sediment availability eventually declines. Material available for transport is limited to the amount introduced by erosional processes. Availability will vary between regions of different geology, land and climate. For example, more material is available during a storm event in regions with easily erodible lithologies, regions with limited vegetation to protect soils or after significant drought conditions. Over the course of the study period, the reach of the Brazos River near Glen Rose experienced exceptional drought conditions. Peak discharge rates for the January 2012 storm event were unprecedented throughout the observation period.

The relationship between suspended sediment concentration and discharge over a specific storm event is explained with a hysteresis curve. This curve is often compared to a hydrograph of the same event to determine at which point sediment transport reached its peak. A hysteresis curve established for the January 2012 storm determined that suspended sediment concentration reached its peak at a discharge of approximately $200 \text{ m}^3\text{s}^{-1}$ along the initial rising limb of the hydrograph (Figure 32). This also marks the point where significant precipitation ceased. The hysteresis curve confirms that an abundance of material was indeed available at the onset of the storm, possibly due to prolonged drought conditions. The loop shows a sharp initial increase in suspended sediment and quickly reaches its maximum before a gradual decline occurs. Discharge continues to increase from $200 \text{ m}^3\cdot\text{s}^{-1}$ to $450 \text{ m}^3\cdot\text{s}^{-1}$ while SSC decreases. The decrease in suspended sediment should be linked to increasing sediment exhaustion over the course of the storm event. The relationship between suspended sediment concentration and discharge displayed in Figure 31 could be strengthened with the inclusion of additional

rising and falling limb data over a range of medium to large storm events. For the purposes of this study, only one major storm event was observed and therefore the majority of the data represents smaller magnitude events with data obtained only along the rising limb or peak of the hydrograph where SSC values are expected to be high.

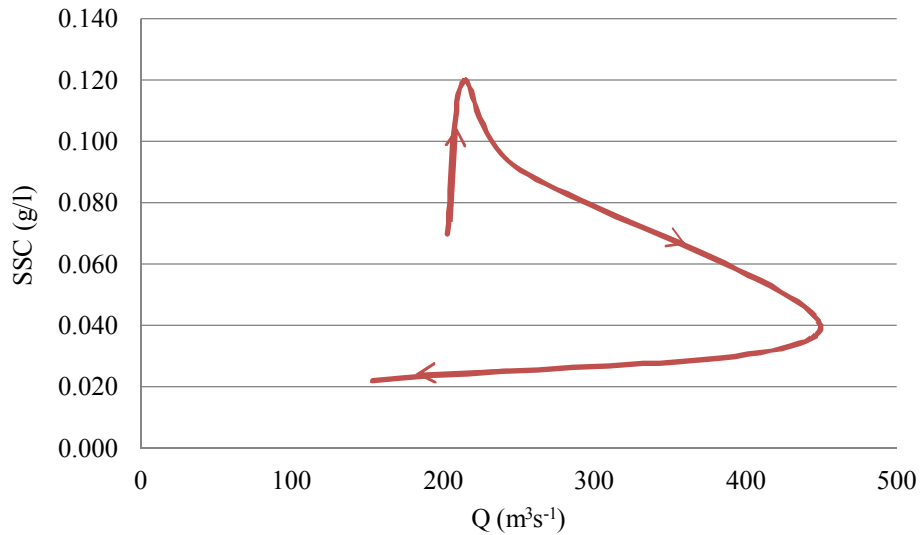


Figure 32. A hysteresis curve for the January 2012 storm event indicates that SSC peaked around $200 \text{ m}^3\text{s}^{-1}$

A stronger relationship exists between suspended sediment flux and discharge (Figure 33). This determines the rate of suspended sediment discharge over a specific discharge. Even though the change in suspended sediment discharge between different observed flow conditions is low, when multiplying it against the specific discharge a strong relationship is established ($R^2 = 0.95$). This determines that 95% of change in suspended sediment can be explained by a change in discharge.

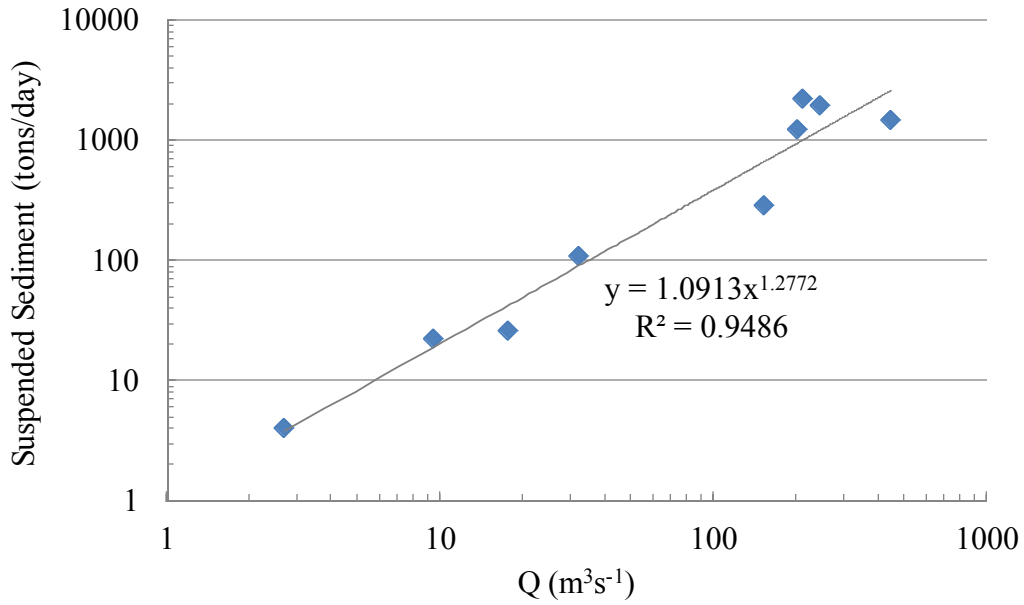


Figure 33. Relationship between suspended sediment flux and discharge

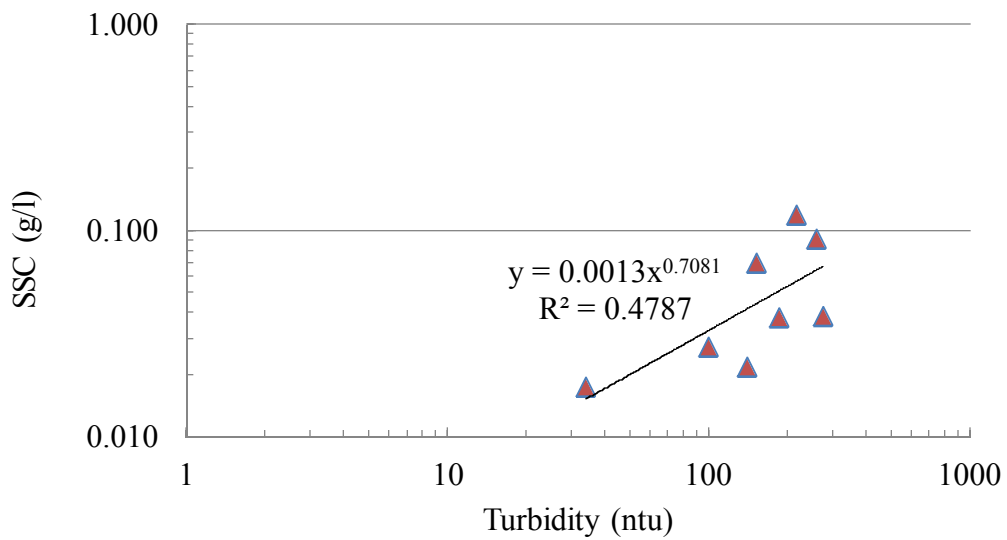


Figure 34. Relationship between turbidity measurements and physical suspended sediment samples obtained during field sampling

In an effort to build a more robust sediment rating curve, the turbidity record may aid to fill gaps of specific flow conditions that were not captured during on site sampling.

As the turbidity probe remained onsite for the entire study period, turbidity measurements may be compared to SSC values obtained over the various sampling events. Figure 34 shows a regression calculation for the relationship between SSC and turbidity establishes a R^2 value of 0.48. The turbidity probe is a highly sensitive measuring tool, and can give faulty readings when the light sensor becomes obstructed by debris. Even though the site was visited regularly and the probe cleaned with each visit, the equipment experienced continuous buildup of organic material especially during summer months when low flow conditions were dominant. A careful interpretation of the entire turbidity record shows extensive scatter in medium to high discharge ranges. The degree of scatter and low correlation does not allow for the collapse of the sediment rating curve and turbidity curve as previously mentioned.

Similarly to suspended load, an average bedload evaluation was made by taking samples at stations across the length of the FM 200 Bridge for the individual flow events. During low flow conditions samples were obtained only at station 1, marking the deepest flow, as transportation rates were expected to be extremely low in shallower areas. Overall, there appears to be large variability in bedload transport rates across the channel. In the field, transport rates were initially obtained as amount of sediment entering the 8cm sampler opening on the channel bed over a 5-minute interval. Load was then converted to a rate per minute over the entire width of the channel. Discharge rates less than $100 \text{ m}^3\text{s}^{-1}$ were characterized by low bedload transport rates. A significant increase of bedload was observed between a discharge increase of $32 \text{ m}^3\text{s}^{-1}$ and $154 \text{ m}^3\text{s}^{-1}$. Calculated bedload transport over the width of the channel for these flow conditions varied from 3 kg/min to 78 kg/min, respectively. A comparison between discharge and

bedload discharge for the different flow events determines a moderately strong relationship with an R^2 of 0.76 (Figure 35). In general, when considering the total sediment load in a river or stream, bedload tends to make up about 10% of the total. With the use of the equations established in the suspended load and bedload curves it was determined that bedload in the Brazos River near Glen Rose makes up approximately 20% of the total load.

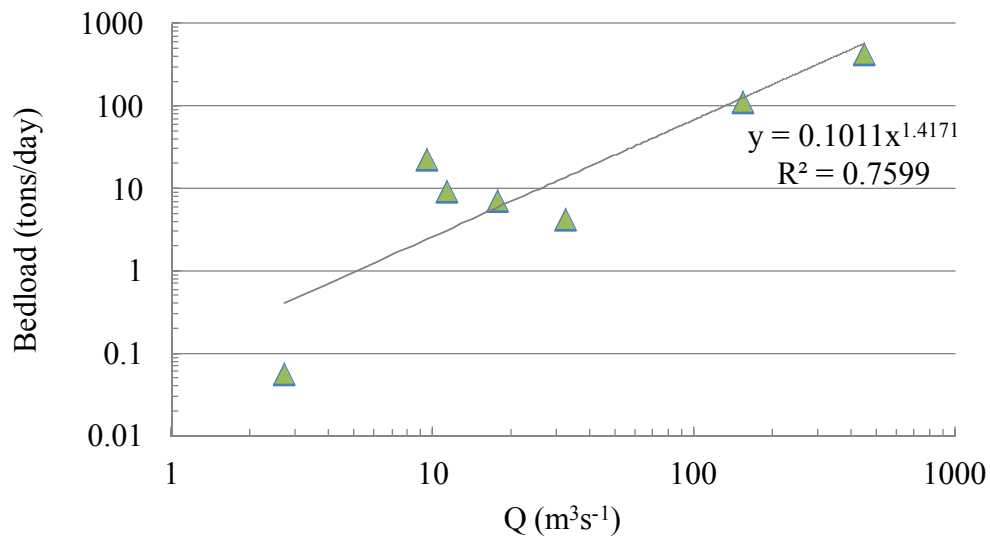


Figure 35. Bedload transportation rates according to variations in Q

CHAPTER 6: CONCLUSION

Even though dams are increasingly important in flood control and water management, they induce large-scale change in a hydrologic system. Changes may be observed by noticeably lower peak discharge rates during seasonal high flow conditions and by alterations in the sediment transport regime. Dams act as a permanent obstruction in a river where downstream sediment transport is interrupted. An imbalance in sediment availability is created above and below a dam structure. In general, if a sediment bypass is not available, sediment is trapped in the reservoir above the dam producing sediment starved water in the reaches directly below the impoundment. A severe reduction in sediment may induce increased scouring in downstream sections as the river attempts to re-equilibrate its sediment load. Scouring of the bed and banks in this region produces a local zone of down cutting and induces a lowering of the stream gradient. The potential for increased sediment mobilization exists in these regions which may result in an increase potential for channel bar development. In a natural system seasonal variation in discharge, low to high flow conditions, produces an overall balance in sediment delivery and removal. However, with the introduction of a dam natural peaks often become dampened or diminished in an effort to control flooding events. Dampening of peak flows decreases a river's overall stream power. Stream power is primarily determined by the slope of the channel and magnitude of discharge. With a decrease in discharge rates, the ability to transport coarse grained material decreases.

These effects were observed in a careful analysis of historic imagery for the study site. Pre-impoundment imagery spanning 20 years showed that bar planform area remained relatively stable over this time span. It therefore suggests that under natural

conditions the rate of sediment removal and delivery must have been in general equilibrium. A significant decrease in planform area was observed in the first post impoundment image; rates varied from 43% to 77% across the channel bar complexes in the study reach. Declines in channel bar areas of this magnitude must be induced by a severe reduction in sediment supply due to the construction of the dam. Alternatively, a second post impoundment image dated to 1984 shows a substantial spike in planform area nearly replenishing pre-impoundment conditions. Accretion rates varied from 20% to 72%. Direct evidence was found for extensive scouring in the reach directly below the dam, suggesting that under altered hydrologic conditions flow was capable of moving substantial amounts of materials.

Climatic variations may further aid in understanding specific planform change. As the study reach is located 40 km below Lake Granbury, effects of the impoundment may become dampened by specific climatic conditions existing between the photograph intervals. Photographic analysis suggests that channel bars are moderately dynamic over a decadal time-frame especially with changes in sediment supply and discharge regimes. For management practices, it is important to understand how channel bars are shaped by short term variations in flow due to fluctuations in seasonal conditions. The study period included a long stretch of severe drought conditions during which the reach experienced mostly low flow conditions. Under these conditions erosive capabilities as well as sediment transport rates remained low and large changes in channel bar morphology were not expected. Surveys obtained over six months of drought conditions validate this assumption. A large storm event, producing discharge rates within the 5% exceedance range, experienced in the later portion of the study period acted as a guideline for

planform area change in the channel bar. A post-storm survey suggests a loss in channel bar area of nearly 33%. This suggests that material within the bar is easily removed and transported as long as stream power is available to do the necessary work. Along with repeated surveying, a sediment record was established for the site which suggests a 14% bedload capacity and an annual sediment flux of 72,207 t/yr.

REFERENCES

- Best, J.L., Ashworth, P.J., Bristow, C.S., Roden, J. (2003) Three-dimensional sedimentary architecture of a large, mid-channel sand braid bar, Jamuna River, Bangladesh. *Journal of Sedimentary Research*, July 2003
- Brazos River Authority. www.Brazos.org
- Dingman, S.L.(2011) *Physical Hydrology*. Waveland Press, Inc. Long Grove, IL
- Downward, S.R., Gurnell, A.M., Brookes, A. (1994) A methodology for quantifying river channel planform change using GIS. Variability in stream erosion and sediment transport (Proceedings of the Canberra Symposium, December 1994) IAHS: 224, 1994
- Dunn, D.D., Haynes, T.H. (2001) Indications and potential sources of change in sand transport in the Brazos River, Texas. US Geologic Survey. Water Resources Investigations Report 01-4057
- Eidse, F. (2005) Rolling River: Analysts Map Apalachicola Changes. *Geoworld* February: 30-33
- Epps, Lawrence Ward (1973) A geologic history of the Brazos River. *Baylor Geological Studies*, 24
- Fryirs, K., Brierly, G. (2001) Variability in sediment delivery and storage along river courses in Bega catchment, NSW, Australia: implications for geomorphic river recovery. *Geomorphology* 38:237-265
- Graf, W.L. (1999) Dam Nation: A geographic census of American dams and their large-scale hydrologic impacts. *Water Resources Research* 35:1305-1311
- Hooke, J.M. (1986) The significance of mid-channel bars in an active meandering river. *Sedimentology* 33: 839-850
- Hudson, P.F., Mossa, J. (1996) Suspended sediment transport effectiveness of the three large impounded rivers, US Gulf Coastal plain. *Environmental Geology* Vol. 32 4:263-273
- Jacobson, R.B., Pugh, A.L. (1995) Riparian-Vegetation Controls on the Spatial Pattern of Stream-Channel Instability, Little Piney Creek, Missouri. Denver: USGS
- Johnson, G. (1997) Instruction manual for USGS sediment observers. USGS 96-431
- Jordan, D.C., Fonstad, M.A. (2005) Two dimensional mapping of river bathymetry and power using aerial photography and GIS on the Brazos River, Texas. *Geocarto International* Vol. 20 3:1-8

- Kondolf, M.G. (1997) Hungry water: effects of dams and gravel mining on river channels. *Environmental Management* Vol. 21 4:533-551
- Kondolf, M.G., Piégay, H. (2003) *Tools in geomorphology*. John Wiley & Sons, Ltd. Chichester, England.
- Leica Scan Station C10 product specifications.
<http://hds.leica-geosystems.com/en/Leica-ScanStation-C10>
- Lisle, T.E. (1982) Effects of aggradation and degradation on riffle-pool morphology in natural gravel channels, Northwestern California. *Water Resources Research* Vol. 18 6: 1643-1651
- Leopold, L.B., M.G. Wolman. *River channel patterns: braiding, meandering, and straight*. Washington D.C.: USGS, 1957
- Marcus, A. W. (2002) Mapping of stream microhabitats with high spatial resolution hyperspectral imagery. *Journal of Geographical systems*. Vol 4: 113-126
- Marcus, A. W., C. J. Legleiter, R. J. Aspinall, J. W. Boardman and R. Crabtree (2003) High spatial resolution hyperspectral mapping of in-stream habitats, depths, and woody debris in mountain streams. *Geomorphology*. Vol 55: 363-380
- O'Connor, J.E., Grant, G.E., Haluska, T.L. (2003) Overview of geology, hydrology, geomorphology, and sediment budget of the Dechutes River Basin, Oregon. *Water Science and Application*
- Phillips, J.D. (2003) Alluvial storage and the long term stability of sediment yields. *Basin Research* 15:153-163
- Phillips, J.D., Slattery, M.C., Musselman, Z.A. (2004) Dam-to-delta sediment inputs and storage in the lower Trinity River, Texas. *Geomorphology* 62:17-34
- Phillips, J.D., Slattery, M.C. (2006) Downstream trends in discharge, slope, and stream power in a lower coastal plain river. *Journal of Hydrology* 334:290-303
- Richards, K. (1982) *Rivers: Form and process in alluvial channels*. Methuen, London, 358pp
- Ritter, D.F., Kochel, R.C., Miller, J.R. (2002) *Process Geomorphology*. McGraw-Hill. New York, NY
- Rosgen, D. *Applied river morphology*. Pagosa Springs: Wildland Hydrology, 1996

- Schumm, S.A. River Adjustment to altered hydrologic regimen – Murrumbidgee River and paleochannels. USGS, 1968
- Slattery, M.C. et al (2010) Holocene sediment accretion in the Trinity River Delta, Texas, in relation to modern fluvial input. *J Soils Sediment* 10:640-651
- Smith, S. (2007) Determining minimum recreational instream flow requirements for a reach of the Brazos River at Glen Rose, Texas. Graduate thesis, Texas Christian University
- Stubblefield, A.P., Reuter, J.E., Dahlgren, R.A., Goldman, C.R (2007) Use of turbidity to characterize suspended sediment and phosphorus fluxes in the Lake Tahoe basin, California, USA. *Hydrological Processes* 21:281-91
- Syvitski, J.M.P et al (2005) Impact of humans on the flux of terrestrial sediment to the global coastal ocean. *Science* 308:376-380
- Texas Natural Resources Information Systems. www.tnris.org
- Trimble GeoXH product specifications. www.trimble.com/mappingGIS
- United States Geological Survey.
http://waterdata.usgs.gov/usa/nwis/uv?site_no=08091000
- Vörösmarty, C.J. et al. (2003) Anthropogenic sediment retention: major global impact from registered river impoundments. *Global Planetary Change* 39:111-126
- Wellmeyer, J.L., Slattery, M.C., Philips, J.D. (2003) Quantifying downstream impacts of impoundment and channel planform, lower Trinity River, Texas. *Geomorphology* 69: 1-13
- Walling, D.E., Fang, D. (2003) Recent trends in the suspended sediment loads of the world's rivers. *Global and Planetary Change* 39:111-12
- Wolman, M.G., J.P. Miller (1960) Magnitude and frequency of forces in geomorphic processes. *Journal of Geology*. Vol 68: 54-74

APPENDIX

Table 1-Appx. Permanent survey control points established in April 2011

Control Point ID	Easting	Northing	Elevation (m)
100	621810.1308	3569706.77	172.289
101	621895.239	3569710.264	172.414
102	621954.3445	3569757.692	172.819
104	622040.9149	3569778.317	172.53
105	622129.3767	3569818.237	172.418
107	622245.3309	3569831.974	172.222
108	622368.8484	3569883.771	173.156
TCU Control 1	622149.451	3569922.726	186.741
TCU Control 2	622248.1869	3569673.07	184.05



Figure 1-Appx. Photographs (2011) of bar inundation trends used to establish an inundation curve

Table 2-Appx. Discharge and gage height information for each photograph

Image Date	Discharge ($\text{m}^3 \cdot \text{s}^{-1}$)	Contemporary Gage Height (m)
3/9/1949	4.53	1.62
2/6/1959	6.63	1.64
2/2/1966	12.8	1.8
7/28/1976	1.33	1.52
2/16/1984	0.37	1.45

Table 3-Appx. Revised bar areas for channel bar 1-B and 1-C

Year	Bar 1- B (m^2)	Gage Height (m)	% inundated	Inundated Area (m^2)	Revised Bar 1-B Area (m^2)
1949	10157	1.62	24.5	2488	12645
1959	7946	1.64	27	2145	10091
1966	5392	1.80	50	2696	8088
1976	3440	1.52	10	344	3784
1984	14135	1.45	0	0	11135
Year	Bar 1-C (m^2)	Gage Height (m)	% inundated	Inundated Area (m^2)	Revised Bar 1-C Area (m^2)
1949	17236	1.62	24.5	4223	21459
1959	14080	1.64	27	3802	17882
1966	16654	1.80	50	8327	24981
1976	5229	1.52	10	523	5752
1984	20376	1.45	0	0	20376

Table 4-Appx. Sediment sampling dates and related discharge measurements

Date	Q ($\text{m}^3 \cdot \text{s}^{-1}$)	Conditions
5/4/2011	17.8	Dam release
7/2/2011	2.7	Low flow
8/13/2011	9.5	Storm event
10/9/2011	32.2	Storm event
11/6/2011	11.3	Dam release
1/25/2011	202.7	Storm event
1/25/2011	213.7	Storm event
1/25/2011	247.6	Storm event
1/26/2011	448.6	Storm event
1/28/2011	153.7	Storm event

Table 5-Appx. Variations in SSC (g/l) at sampling stations. Highest concentrations are shown in yellow.

Q (m³·s⁻¹)	1	2	center	3	4
2.7	0.015			0.020	
9.5	0.030	0.035	0.030	0.035	0.010
17.8	0.020	0.020	0.010	0.010	0.025
32.2	0.020	0.035	0.040	0.060	0.060
153.7	0.020	0.030	0.010	0.020	0.030
202.7	0.060	0.070	0.080	0.060	0.080
213.7	0.120	0.100	0.120	0.130	0.120
247.6	0.100	0.070	0.070	0.100	0.120
448.6	0.030	0.040	0.040	0.030	0.050

Table 6-Appx. Variations in bedload yield (g/5min) at bridge sampling stations.

Q (m³·s⁻¹)	1	2	center	3	4
2.7	No yield				
9.5	92.3				
11.3	37.2				
17.8	28.5				
32.2	10.0		32.9		7.6
153.7	336.0		846.0		160.0
448.6	3322.0		858.0		1098.0



Figure 2-Appx. 1949 photograph of study site (1:10,000)



Figure 3-Appx. 1959 photograph of study site (1:10,000)



Figure 4-Appx. 1966 photograph of study site (1:10,000)



Figure 5-Appx. 1976 photograph of study site (1:10,000)



Figure 6-Appx. 1984 photograph of study site (1:10,000)



Figure 7-Appx. 1976 photograph of Lake Granbury and De Cordova Bend Dam (1:24,000)



Figure 8-Appx. 1958 photography of Brazos River at the current location of De Cordova Bend Dam

VITA

Personal Background	Maartje Lucia Klara Melchiors Born September 18, 1982 in Deurne, Netherlands Daughter of Lauran and Marian Melchiors Married James Elliott Sykes, August 23, 2007 One child
Education	Bachelor of Arts, Art History, University of Houston Houston, 2004 Bachelor of Arts, Geology, University of Vermont Burlington, 2008 Master of Science, Geology, Texas Christian University Fort Worth, 2012
Experience	Teaching Assistantship, Texas Christian University 2010-2012 Research Assistant, TCU Wind Research Initiative 2011-2012 Research Assistant, Dept. of Geography, University of Vermont 2007-2009
Memberships	Association for Environmental and Engineering Geologists Association of American Geographers

ABSTRACT

ASSESSING SEDIMENT DYNAMICS AND CHANNEL BAR RESPONSE IN THE BRAZOS RIVER NEAR GLEN ROSE, TEXAS

by Maartje L.K. Melchior
School of Geology, Energy & the Environment
Texas Christian University

Thesis advisor: Dr. Michael Slattery
Professor of Environmental Science, Director of the Institute of Environmental Studies

This thesis presents the results of a one year study examining sediment transport rates and channel bar morphology in the Brazos River near Glen Rose, Texas. All observations were made along a study site located below De Cordova Bend Dam at Lake Granbury. The project aimed at understanding the historic migration patterns of channel bars pre- and post-dam construction. This was achieved through the analysis of aerial photography and ArcGIS. Additionally, the project monitored present annual sediment flux and channel bar response to understand short term changes within the system. Suspended load and bedload were measured over a range of flow conditions, and channel bars surveyed continuously to capture seasonal variability. Channel bar development is largely controlled by stream capacity and the availability of sediment, and therefore channel bars within our study area represent key observational features for understanding the current dynamics of the fluvial system.